

University of Windsor

## Scholarship at UWindor

---

Electronic Theses and Dissertations

Theses, Dissertations, and Major Papers

---

1-1-1963

### Sensitized fluorescence in potassium vapour at low densities.

George D. Chapman  
*University of Windsor*

Follow this and additional works at: <https://scholar.uwindsor.ca/etd>

---

#### Recommended Citation

Chapman, George D., "Sensitized fluorescence in potassium vapour at low densities." (1963). *Electronic Theses and Dissertations*. 6325.  
<https://scholar.uwindsor.ca/etd/6325>

This online database contains the full-text of PhD dissertations and Masters' theses of University of Windsor students from 1954 forward. These documents are made available for personal study and research purposes only, in accordance with the Canadian Copyright Act and the Creative Commons license—CC BY-NC-ND (Attribution, Non-Commercial, No Derivative Works). Under this license, works must always be attributed to the copyright holder (original author), cannot be used for any commercial purposes, and may not be altered. Any other use would require the permission of the copyright holder. Students may inquire about withdrawing their dissertation and/or thesis from this database. For additional inquiries, please contact the repository administrator via email ([scholarship@uwindsor.ca](mailto:scholarship@uwindsor.ca)) or by telephone at 519-253-3000ext. 3208.

SENSITIZED FLUORESCENCE IN POTASSIUM VAPOUR AT LOW DENSITIES

BY

GEORGE D. CHAPMAN

A Thesis

Submitted to the Faculty of Graduate Studies through the Department  
of Physics in Partial Fulfillment of the Requirements for  
the Degree of Master of Science at Assumption  
University of Windsor.

Windsor, Ontario

1963

UMI Number: EC52504

## INFORMATION TO USERS

The quality of this reproduction is dependent upon the quality of the copy submitted. Broken or indistinct print, colored or poor quality illustrations and photographs, print bleed-through, substandard margins, and improper alignment can adversely affect reproduction.

In the unlikely event that the author did not send a complete manuscript and there are missing pages, these will be noted. Also, if unauthorized copyright material had to be removed, a note will indicate the deletion.

**UMI<sup>®</sup>**

---

UMI Microform EC52504

Copyright 2008 by ProQuest LLC.

All rights reserved. This microform edition is protected against unauthorized copying under Title 17, United States Code.

ProQuest LLC  
789 E. Eisenhower Parkway  
PO Box 1346  
Ann Arbor, MI 48106-1346

AAX 5139

APPROVED

*R. Thibert*  
.....  
Dr. R. Thibert

*N. Hedgecock*  
.....  
Dr. N. Hedgecock

*L. Krause*  
.....  
Dr. L. Krause  
(Supervisor)

73716

# ABSTRACT

The sensitized fluorescence of potassium vapour, induced by potassium - potassium and potassium - argon collisions, was investigated for the first time at low potassium densities to determine the efficiency of collisions of the second kind in these systems. The collision numbers were found to vary linearly with atomic density in both types of collisions. In both systems, the probabilities of the transitions  $4^2P_{3/2} \rightarrow 4^2P_{1/2}$  and  $4^2P_{1/2} \rightarrow 4^2P_{3/2}$  were found to be identical at low atomic densities. The cross section for potassium - potassium collisions at low pressure is given by

$$Q = 3.30 \times 10^{-13} \sqrt{T}$$

$$\text{or } Q = 6.60 \times 10^{-12} \text{ cm}^2 \text{ at } 400^\circ \text{K}$$

Similarly, for potassium - argon collisions:

$$Q = 7.25 \times 10^{-15} \sqrt{T}$$

$$\text{or } Q = 1.4 \times 10^{-14} \text{ cm}^2 \text{ at } 373^\circ \text{K.}$$

At higher pressures, the probability of an upward transition was found to be greater than the probability of a downward transition, and the cross sections were found to vary inversely with pressure.

For the potassium - argon collisions at pressures above 20 Torr:

$$Q_1 (4^2P_{1/2} \rightarrow 4^2P_{3/2}) = \left( 8.70 \times 10^{-17} + \frac{3.15 \times 10^{-15}}{P} \right) \sqrt{T}$$

$$Q_2 (4^2P_{3/2} \rightarrow 4^2P_{1/2}) = \left( 5.14 \times 10^{-17} + \frac{2.52 \times 10^{-15}}{P} \right) \sqrt{T}$$

or at 373 K and 200 Torr

$$Q_1 = 1.98 \times 10^{-15} \text{ cm}^2$$

$$Q_2 = 1.23 \times 10^{-15} \text{ cm}^2$$

The identity of  $Q_1$  and  $Q_2$  at low pressures is explained on the

basis of conservation of the component of the total angular momentum of the colliding atoms along the collision axis.

#### ACKNOWLEDGEMENTS

I should like to express my appreciation for the assistance afforded me in the preparation of this thesis by Dr. L. Krause, under whose direction this investigation was conducted. My thanks also to the National Research Council of Canada which provided the bursary that made this research financially feasible for me.

# TABLE OF CONTENTS

	Page
ABSTRACT . . . . .	11
ACKNOWLEDGEMENTS . . . . .	iv
I. INTRODUCTION . . . . .	1
Resonance Fluorescence in Alkali Metal Vapours	1
Sensitized Fluorescence . . . . .	2
II. THEORETICAL . . . . .	5
III. EXPERIMENTAL . . . . .	12
A The Apparatus . . . . .	12
1. The Light Source . . . . .	14
2. The Monochromator . . . . .	20
3. The Fluorescence Cell and The Furnace . . . . .	20
4. The Evacuating and Filling System . . . . .	27
5. The Recording Spectrometer . . . . .	29
B The Optical Line Up . . . . .	29
IV. RESULTS AND DISCUSSION . . . . .	32
Sensitized Fluorescence in Potassium Vapour . . . . .	32
The Total Intensity of Fluorescence in Potassium Vapour . . . . .	48
Sensitized Fluorescence Induced by Potassium - Argon Collisions . . . . .	52
V. THE RELATIONSHIP BETWEEN $Q_1$ AND $Q_2$ FOR INELASTIC COLLISIONS . . . . .	61
VI. CONCLUSIONS . . . . .	63
BIBLIOGRAPHY . . . . .	66
VITA AUCTORIS . . . . .	67



# LIST OF TABLES

Table		Page
1	Intensity Ratios in Sensitized Fluorescence Induced by Potassium - Potassium Collisions . . . . .	34
2	Collision Numbers in Sensitized Fluorescence Induced by Potassium - Potassium Collisions . . . . .	41
3	Total Intensity in Sensitized Fluorescence Induced by Potassium - Potassium Collisions . . . . .	49
4	Intensity Ratios in Sensitized Fluorescence Induced by Potassium - Argon Collisions . . . . .	54
5	Collision Numbers in Sensitized Fluorescence Induced by Potassium - Argon Collisions . . . . .	57

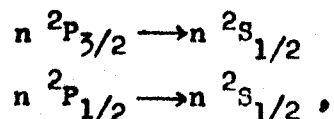
# LIST OF DIAGRAMS

Figure		Page
1	The Arrangement of the Apparatus . . . . .	13
2	The Radio Frequency Lamp . . . . .	13
3	The Radio Frequency Oscillator Circuit . . . . .	16
4	The Heater Control Circuit . . . . .	17
5	Detail of the Fluorescence Cell . . . . .	21
6	Detail of the Oven Construction - Lateral View . .	24
7	Detail of the Oven Construction - Plan View . . .	24
8	The Wiring of the Oven Circuits . . . . .	26
9	The Vacuum and Filling System . . . . .	28
10	The Variation of $\gamma_1$ With Potassium Vapour Pressure .	36
11	The Variation of $\gamma_2$ With Potassium Vapour Pressure .	36
12	A Semi - Logarithmic Plot of $\gamma_1$ and $\gamma_2$ Against Potassium Vapour Pressure . . . . .	38
13	The Variation of $\gamma$ , $Z$ , and $Q$ With Potassium Vapour Pressures at Low Potassium Densities . . . . .	43
14	A Semi - Logarithmic Plot of $Z_1$ and $Z_2$ Against Potassium Vapour Pressures . . . . .	47
15	The Variation of the Total Fluorescent Intensity With Potassium Vapour Pressure . . . . .	50
16	The Variation of $\gamma_1$ and $\gamma_2$ With Argon Pressure . .	55
17	A Semi - Logarithmic Plot of $\gamma_1$ and $\gamma_2$ Against Argon Pressure . . . . .	56
18	The Variation of $Z_1$ and $Z_2$ With Argon Pressure . .	58
19	The Variation of $Z_1$ and $Z_2$ With Argon Pressure at Low Argon Densities . . . . .	60

## I INTRODUCTION

### Resonance Fluorescence in Alkali Metal Vapours.

If atoms in the ground state are irradiated with light of frequency  $\nu$  and, in returning to the ground state, reemit light of the same frequency, the emitted light is termed resonance radiation. This means that if an atom possesses some state from which there exists but one downward transition, this state is a resonance state. The alkali metals possess two such resonance states whose corresponding downward transitions may be represented as :



where  $n$  is the principal quantum number of the metal concerned. The spectral lines arising from these transitions are known as the D lines.

R. W. Wood (1905) first observed resonance fluorescence with sodium and originated the term resonance fluorescence. He noticed that when a cone of resonance radiation was made incident on a sample of alkali vapour, it was sharply defined by a cone of fluorescent light. As the vapour density was increased the fluorescent light expanded to fill the fluorescence vessel; this condition became known as volume fluorescence. The effect is due to trapping or imprisonment of radiation; photons are emitted and reabsorbed many times before leaving the vessel, exciting those atoms lying outside the incident cone. As the vapour density was further increased, the radiation was eventually confined to a shallow layer at the point where the incident radiation entered the fluorescence vessel. This was surface fluorescence. All of these phases of radiation diffusion may be observed

with either or both of the D lines.

### Sensitized Fluorescence.

Let us consider a mixture of atoms in vapour phase in which the atoms may exist in excited states lying within a small energy gap  $\Delta W$  of each other. If the mixture is irradiated with light of a wavelength suitable for the excitation of the atom with the higher energy level, then the fluorescent light may contain components due to the normal decay of both atomic species. This reradiation of a wavelength different from that in the exciting beam is called sensitized fluorescence.

This effect is due to inelastic collisions between the two atomic species during which radiationless energy transfer takes place. The energy defect appears as increased relative kinetic energy between the colliding atoms. The effect was verified by Cario and Franck (1922) in their experiments with a mixture of mercury and thallium vapours. The collisions of the second kind are defined according to Franck's extension of the terminology of Klein and Rosseland to include not only the collisions of excited atoms with slow electrons to produce deexcited atoms and fast electrons, but also collisions between excited atoms and atoms in the ground state. Collisions of the first kind are collisions between ground state atoms and fast electrons which give rise to slow electrons and excited atoms or ions.

Kinetic energy can also bridge the gap between lower and higher states when the atomic mixture is irradiated with light which will excite the atoms possessing the lower excited state. Thus collisions of the second kind may cause radiationless energy transfers between atoms with energy levels which are within the mean thermal kinetic

energy, (kT), of one another.

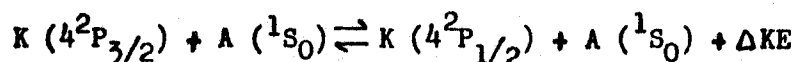
This argument can be readily extended to atoms of a single kind with two resonance levels, such as those of the alkali metals.

The energy transfer in a collision between a potassium atom in a resonance state and one in the ground state can be represented by



Inelastic collisions between two atoms are most efficient when the least energy is converted into kinetic energy, or vice versa. (J. Franck, 1929). Beutler and Josephy (1929) first succeeded in demonstrating this principle by experiments with the sensitized fluorescence in sodium vapour. They explained it on the basis of a quantum mechanical resonance between the two states.

Collisions between alkali atoms and inert gas atoms may also produce sensitized fluorescence as represented by the following expression involving potassium and argon.



Sensitized fluorescence may be used to determine the total cross sections for inelastic collisions in alkali metal vapours and in mixtures of alkali metals and inert gases. These cross sections may be regarded as criteria of the efficiency of the energy transfer. The alkali metals lend themselves to these studies since there are no energy levels lying close to the resonance levels, which would interfere with the energy transfer. The energy gap between the resonance states is relatively small ( $57 \text{ cm}^{-1}$  for potassium) and energy transfers, in principle, take place even at room temperature.

The imprisonment of radiation presents a most difficult obstacle to the study of inelastic collisions in these systems. As the vapour

density of potassium increases, a photon may be absorbed and reemitted many times before it leaves the vapour and is detected. This causes an artificial increase in the lifetimes of the excited states. There have been several attempts at theoretical compensation for these diffusion effects, notably those of Compton (1923) who attacked the problem in analogy to molecular diffusion, and Milne (1926) who further developed Compton's approach. Holstein (1947) treated radiation imprisonment in terms of the probability that a photon would be absorbed while traversing a known thickness of gas. Barrat (1959) carried out extensive theoretical and experimental investigations of diffusion of mercury resonance radiation. Holstein's theory was adapted by Hoffmann and Seiwert (1961) who used it to compensate for radiation diffusion in potassium systems.

None of these theories lend themselves particularly well to the correction of experimental data for the effects of radiation imprisonment without necessitating various assumptions about the geometry of the fluorescence cell. It is therefore the purpose of this investigation to observe sensitized fluorescence in potassium at vapour densities at which diffusion of radiation becomes insignificant. In this way, it should be possible to eliminate the need for theoretical corrections and to obtain true cross sections for collisions of the second kind.

## II THEORETICAL

The rate of energy transfer in atomic collisions may be expressed statistically as a function of the relative kinetic energy of the impacting atoms. This transfer rate is the total cross section for an interaction at a specific temperature and may be defined in the following manner:

$$Q(T) = \int_0^{\infty} q(E) f_T(E) dE, \quad (1)$$

where  $E$  is the relative kinetic energy of the colliding atoms and  $q(E)$  is the cross section for a collision between two atoms whose relative kinetic energy lies between  $E$  and  $E + dE$ .  $f_T(E)dE$  is the probability that at a temperature  $T$  the kinetic energy of the relative motion of the colliding atoms will lie between  $E$  and  $E + dE$ , defined in Maxwell - Boltzmann statistics as:

$$f_T(E)dE = \frac{2\sqrt{E}}{\sqrt{\pi}(kT)^{3/2}} \exp - (E/kT) dE. \quad (2)$$

The collision number,  $Z(T)$ , the average number of collisions per atom per second which result in energy transfer, is defined as:

$$Z(T) = N \sqrt{2/M} \int_0^{\infty} q(E) \sqrt{E} f_T(E) dE, \quad (3)$$

where  $M$  is the reduced mass,  $N$  is the atomic density of ground state atoms in atoms /cc, which approximately equals the overall density.

Since  $Q(T)$  and  $Z(T)$  vary similarly with  $T$  as  $q(E)$  does with kinetic energy, equations (1) and (3) may be combined to give,

$$\begin{aligned} &\text{substituting } E = \frac{M V_r^2}{2} \text{ in (3),} \\ Q(T) &= \frac{Z(T)}{N V_r}, \end{aligned} \quad (4)$$

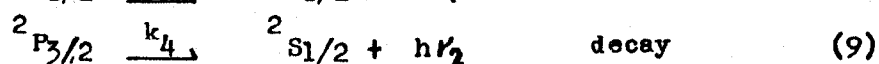
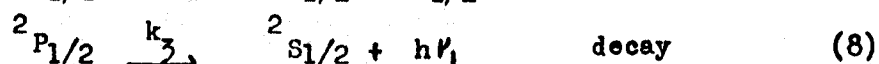
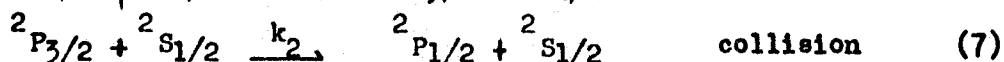
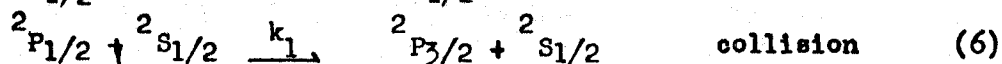
where  $V_r$  is the average relative velocity of the colliding atoms:

$$V_r = \sqrt{\frac{8kT}{\pi M}}$$

The collision numbers  $Z(T)$  are obtained directly from experimental data and, using equation (4), they in turn yield the cross sections.

If it is assumed that the fluorescing vapour is being continually irradiated by one of the potassium D lines of constant intensity, then the sample exists in a state of dynamic equilibrium in which the rate of deexcitation of any atomic state is just equal to its rate of formation. Then the methods of reaction kinetics may be employed to describe this steady-state condition.

Let us consider first that the sample is being irradiated by the 7699 Å line of potassium ( $4^2P_{1/2} \rightarrow 4^2S_{1/2}$ ). It is assumed for the moment that there is no radiation diffusion taking place. Under these conditions the processes existing for the excitation and deexcitation of the  $^2P_{1/2}$  level may be represented by the following relations:





In these equations,  $k_0 - k_6$  represent the rates of the transitions. These relationships are more usefully defined in terms of the instantaneous density of atoms in each of the three possible atomic states. Accordingly, let

$N_1$	density of atoms in	$^2P_{1/2}$ state
$N_2$	" " " " " " "	$^2P_{3/2}$ state
$N_0$	" " " " " " "	$^2S_{1/2}$ state

This allows equations (5) - (11) to be rewritten in terms of the numbers of atoms in each state, whose instantaneous densities depend on several competing processes.

Equation (5) represents excitation by incident radiation. Equations (6) and (7) describe collisions of the second kind, while (8), (9), (10), (11) represent normal decay and quenching of the excited states against the cell walls. The rate constants  $k_3$  and  $k_4$  are equal to the reciprocal of the mean lifetime of the of the excited state involved. Since these lifetimes  $\tau_1$  and  $\tau_2$  are approximately equal,  $k_3 = k_4 = 1/\tau$ . Similarly, the first order quenching termination rate constants  $k_5$  and  $k_6$  are equal, (ie)  $k_5 = k_6 = \gamma$ . The rate constant  $k_0$  is equal to the quantum yield  $\phi_1$  in atoms excited per Einstein multiplied by the absorbed incident radiation  $I_{\text{abs}}$ . For the sake of brevity set  $\phi_1 I_{\text{abs}} = S_1$ .

Under steady - state conditions, the mass action law yields the following equations:

$$\frac{dN_1}{dt} = 0 = S_1 - k_1 N_1 N_0 + k_2 N_2 N_0 - k_3 N_1 - k_5 N_1 \quad (12)$$

$$\frac{dN_2}{dt} = 0 = k_1 N_1 N_0 - k_2 N_2 N_0 - k_4 N_2 - k_6 N_2 \quad (13)$$

$N_0$  is very large with respect to  $N_1$  and  $N_2$  and may be considered constant.

Set  $k_1 N_0 = Z_1$  and  $k_2 N_0 = Z_2$ . Equations (12) and (13) become:

$$0 = S_1 - Z_1 N_1 + Z_2 N_2 - (1/\gamma + \delta) N_1 \quad (14)$$

$$0 = Z_1 N_1 - Z_2 N_2 - (1/\gamma + \delta) N_2 \quad (15)$$

which immediately gives

$$S_1 = \frac{N_1 + N_2}{1/\gamma + \delta} \text{ as expected for first order terminal reactions.}$$

If the 7665 Å line is made incident on the sample, two more equations may be obtained in a manner similar to that used to obtain (14) and (15),

$$0 = S_2 + Z_1 N_1 - Z_2 N_2 - (1/\gamma + \delta) N_2 \quad (16)$$

$$0 = -Z_1 N_1 + Z_2 N_2 - (1/\gamma + \delta) N_1 \quad (17)$$

From equations (15) and (17)

$$\frac{Z_1}{Z_2 - 1} = \frac{(1/\gamma + \delta) N_2}{(1/\gamma + \delta) N_1} = \eta_2 \quad (18)$$

$$\frac{Z_2}{Z_1 - 1} = \frac{(1/\gamma + \delta) N_1}{(1/\gamma + \delta) N_2} = \eta_1 \quad (19)$$

If the quenching rate is negligibly small compared with the normal decay rate  $1/\gamma$ , then

$$\eta_2 = \frac{I_2}{I_1} = \frac{(1/\gamma) N_2}{(1/\gamma) N_1} \quad .$$

$\eta_1$  is similarly defined. Solving (18) and (19) for  $Z_1$  and  $Z_2$ :

$$Z_1 = \frac{1 + \eta_1}{\gamma(1/\eta_2 - \eta_1)} \quad (20)$$

$$Z_2 = \frac{1 + \eta_2}{\gamma(1/\eta_1 - \eta_2)} \quad (21)$$

Experimental data are obtained in the form of intensity ratios  $\gamma_1$  and  $\gamma_2$  which, using equations (20) and (21), give the collision numbers  $Z_1$  and  $Z_2$ . The collision numbers, inserted in equation (4), yield the required cross sections.

The termination constant  $(1/\tau + \delta)$  critically affects the evaluation of cross sections. If an effective or experimentally observed lifetime is defined as  $\tau_E$  where  $\frac{1}{\tau_E} = (1/\tau_D + \delta)$  ( $\tau_D$  is the lifetime of the excited state as observed under conditions of radiation diffusion) then:

$$\tau_E = \frac{\tau_D}{1 + \tau_D \delta} \quad (22)$$

From (22) it is obvious that in order to observe a "true" lifetime and therefore a correct collision number, the quenching rate must be zero or at least vanishingly small.

$$\text{Then } \tau_E = \tau_D \quad (23)$$

Equation (23) indicates that radiation diffusion must be absent for  $\tau_E$  to be the true lifetime. These are the two major assumptions which affect the validity of equations (4), (20) and (21); there must be no quenching or diffusion of radiation. Quenching tends to decrease the apparent lifetime, altering the collision numbers and cross sections. In addition, if radiation is imprisoned,  $\tau_1$  no longer equals  $\tau_2$ , since the absorption coefficient for the 7665Å line is twice that for the 7699Å line.

If equation (4) is reduced to a function of temperature and pressure by the introduction of appropriate conversion factors,

the equation

$$Q(T) = \frac{3.15 \ Z(T) \ \sqrt{T} \times 10^{-23}}{P(\text{Torr})} \quad (24)$$

holds for potassium - potassium collisions. This relation is virtually unchanged for potassium - argon collisions since the atomic masses of potassium and argon are very nearly equal: 39.1 and 39.9 units respectively.

For  $Q(T)$  to remain finite, it is required that  $\sqrt{T} Z(T)$  go to zero more rapidly than the pressure. However, before the question of whether or not  $Q(T)$  remains finite arises, the concept of pressure as a thermodynamic effect becomes meaningless. Moreover since it has been previously postulated that  $Q(T)$  and  $Z(T)$  vary similarly with  $T$  as does  $Q(T)$  with  $(E)$  in order to establish the approximation to  $Q(T)$  given as equation (4), there is the implied restriction that there must be a statistical array of atoms in the sample under consideration. This restriction as well as the restriction on  $Z(T)$  with regard to quenching and radiation imprisonment, sets the limits of the validity of equations (4) and (24). This equation applies strictly at pressures below those required for radiation imprisonment and yet high enough to maintain an atomic density to which Maxwell - Boltzmann statistics may be applied and in the absence of quenching.

The point at which radiation imprisonment begins is relatively easy to find from plots of total fluorescent intensity. However, the lower limit of validity is not so obvious.

It can be seen from equations (20) and (21) that if the

theoretical statistical population ratios are ever attained, ( for potassium,  $\frac{N_2}{N_1} = 2.0$   $\frac{N_1}{N_2} = 0.5$  ) then the collision numbers and hence the collision cross sections go to infinity. This is due to the effects of radiation diffusion which is required for the establishment of these ratios. Energy is transferred from one level to the other at rates which become indeterminate.

The above statement does not contradict the contention that radiation diffusion increases the apparent lifetimes and decreases the corresponding cross sections. In this case,  $\mathcal{T}$  in equations (20), and (21) is a constant which is the mean lifetime of an isolated atom. When radiation diffusion sets in, the increase in the apparent lifetimes is felt as a shift in the values in the ratios  $\gamma_1, \gamma_2$ , since it was assumed that the lifetime  $\mathcal{T}$  was a constant in the equations for  $Z(T)$ .

If we wished to find the real values for  $Z(T)$  when radiation is imprisoned, it must be assumed that  $\mathcal{T}$  is a variable which increases roughly at the same rate as the ratio  $\frac{1 + \gamma_1 \text{ or } 2}{1/\gamma_2 \text{ or } 1 - \gamma_1 \text{ or } 2}$ . This procedure would, in principle, yield real, finite cross sections at these atomic densities. In practice, however, the relation of experimental data to theory would lead to precisely the assumptions and approximations which we are trying to avoid by working in the absence of radiation imprisonment.

### III EXPERIMENTAL

#### A The Apparatus.

The arrangement of the experimental apparatus is illustrated in figure (1). An alkali vapour lamp was used as a source of the potassium resonance doublet. The light from this source passed into a grating monochromator which served to separate the components of the doublet. Monochromatic light was then brought to a focus in a fluorescence cell contained in an electric furnace. An evacuation and filling system was provided to evacuate the fluorescence cell and to admit to it controlled quantities of inert gases. The fluorescent light emitted by the potassium atoms in the cell was analyzed and recorded by a recording spectrometer. The apparatus shown in figure (1) includes the following components:

- A Light source
- B Monochromator
- $L_1$  f/1.0 lens of focal length 5.5 cm
- $L_2$  f/2.9 lens of focal length 26 cm
- C Fluorescence cell in oven
- $L_3$  f/1.11 lens of focal length 10 cm
- D Spectrometer
- E Photomultiplier in cryostat
- F Electrometer
- G Strip recorder

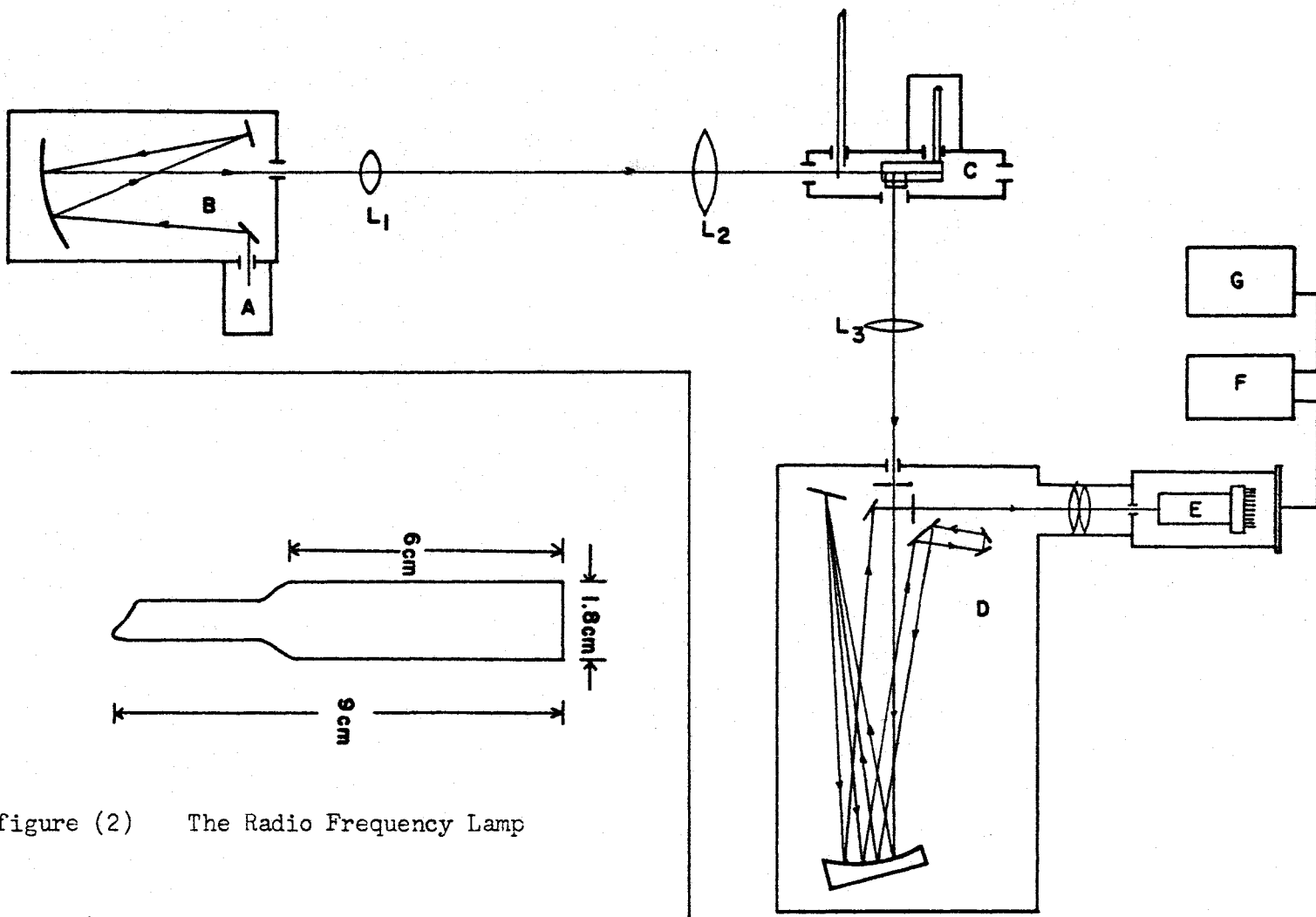


figure (2) The Radio Frequency Lamp

figure (1) The Arrangement of the Apparatus

## 1 The Light Source.

The ideal source of resonance radiation for the purpose of this investigation would be one with a steady, high intensity, no self-reversal and with as narrow a line width as possible.

Commercial potassium vapour lamps, manufactured by Osram, were at first used as light sources. These lamps have the advantage of extreme simplicity of operation and compactness. However, they emit low intensity in the potassium D lines and exhibit considerable line broadening and self-reversal. It was also found that the  $7665\text{\AA}$  component of the resonance doublet fluctuated by 10 - 12% in a sinusoidal manner with a period of five minutes. All attempts to eliminate this effect by altering the thermal environment or electrical characteristics of the lamp were unsuccessful.

In an attempt to increase total intensity and to eliminate the fluctuation of the  $7665\text{\AA}$  line, a modified version of the radio frequency source described by Gerard (1961) was constructed. Although the intensity of this source was about 20 times that of the Osram lamps, the fluctuation of the  $7665\text{\AA}$  component was exactly the same.

A series of experiments with both types of lamp indicated that the intensity fluctuation was due to variations in the wings of the line, no such fluctuation appears in the fluorescent light emitted by a sample of potassium irradiated with light from either source. This might explain why only the  $7665\text{\AA}$  varied since it has the more elaborate hyperfine structure of the two multiplet lines.

In addition, the total fluorescent intensities produced by both



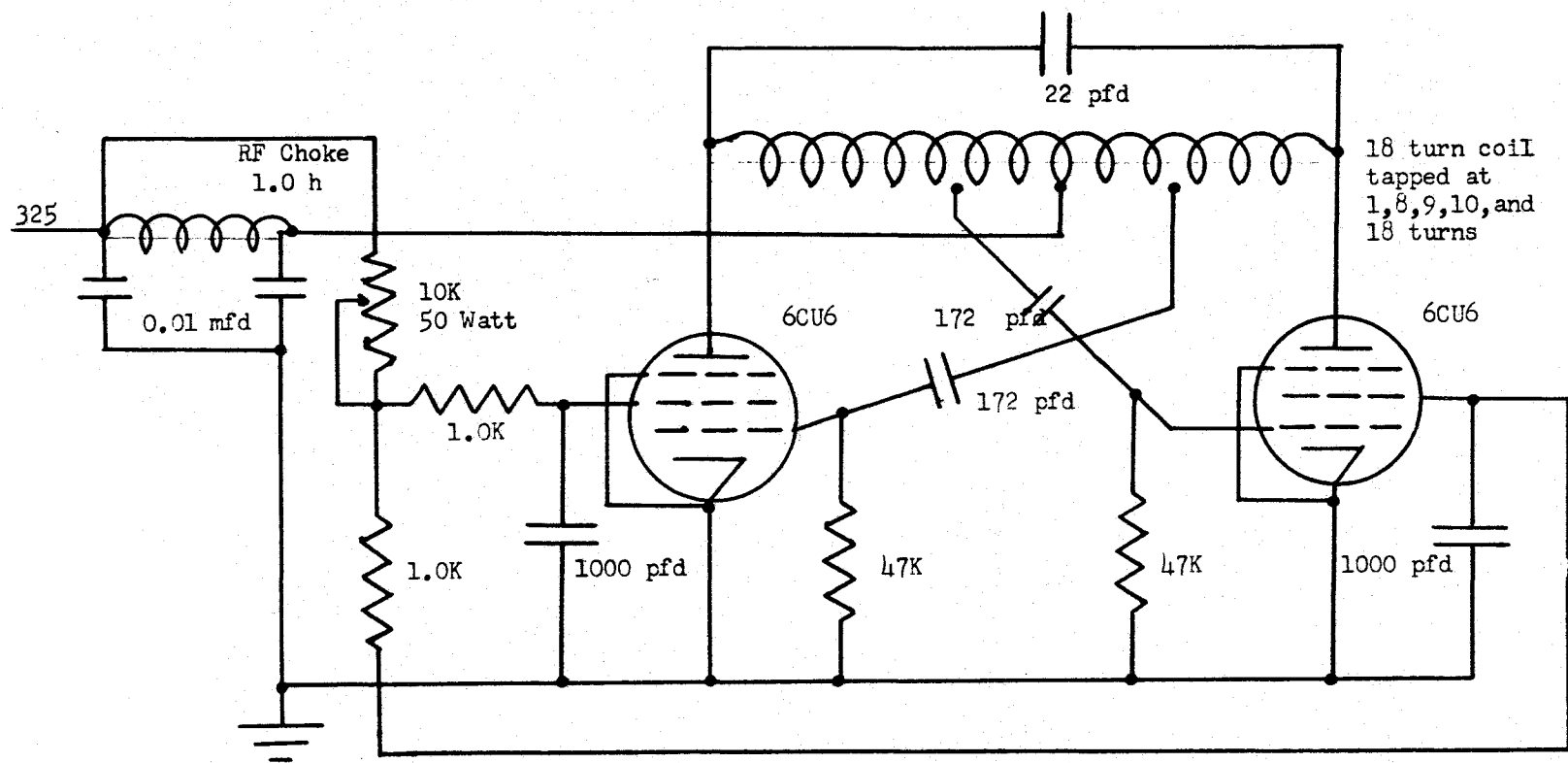
lamps at various atomic densities indicated that the lines produced by the Osram lamp were broader and more self - reversed than the lines produced by the radio frequency source.

The RF lamp itself is shown in fig (2). It is made of pyrex glass and contained about 0.5 gm of potassium which had been distilled four times under vacuum to purify it. About 2.0 Torr of commercial grade argon was also admitted to the lamp to carry the RF discharge until the potassium was vapourized. Soft, alkali resistant glasses were used to limit the corrosive action of the hot potassium vapour on the lamp, but proved unable to resist the thermal shocks of lamp operation.

The base of the lamp was mounted in a block of asbestos containing a resistance wire heater to control the potassium vapour pressure. An 18 - turn RF coil surrounded the body of the lamp. The coil was part of the tank circuit of a radio frequency power oscillator. When the tank circuit is properly tuned, the lamp is heated to about  $300^{\circ}\text{C}$  by dielectric losses in the glass.

The lamp circuits consist of two parts; the radio frequency oscillator, fig (3), and the temperature controller, fig (4).

The RF oscillator is of a push - pull type and is operated in class C. It is powered by a Lambda Regulated Power Supply Model C-482M. Since the feedback path for each half of the circuit involves a beam tetrode which introduces a constant phase shift of  $180^{\circ}$ , the tank circuit is the only frequency determining element for lower frequencies. Above 20 mcs inter-electrode capacities also affect the operating frequency. Power to the coil is regulated by the 10K



All resistors 2.0 Watt unless otherwise specified.

figure (3) The Radio Frequency Oscillator Circuit

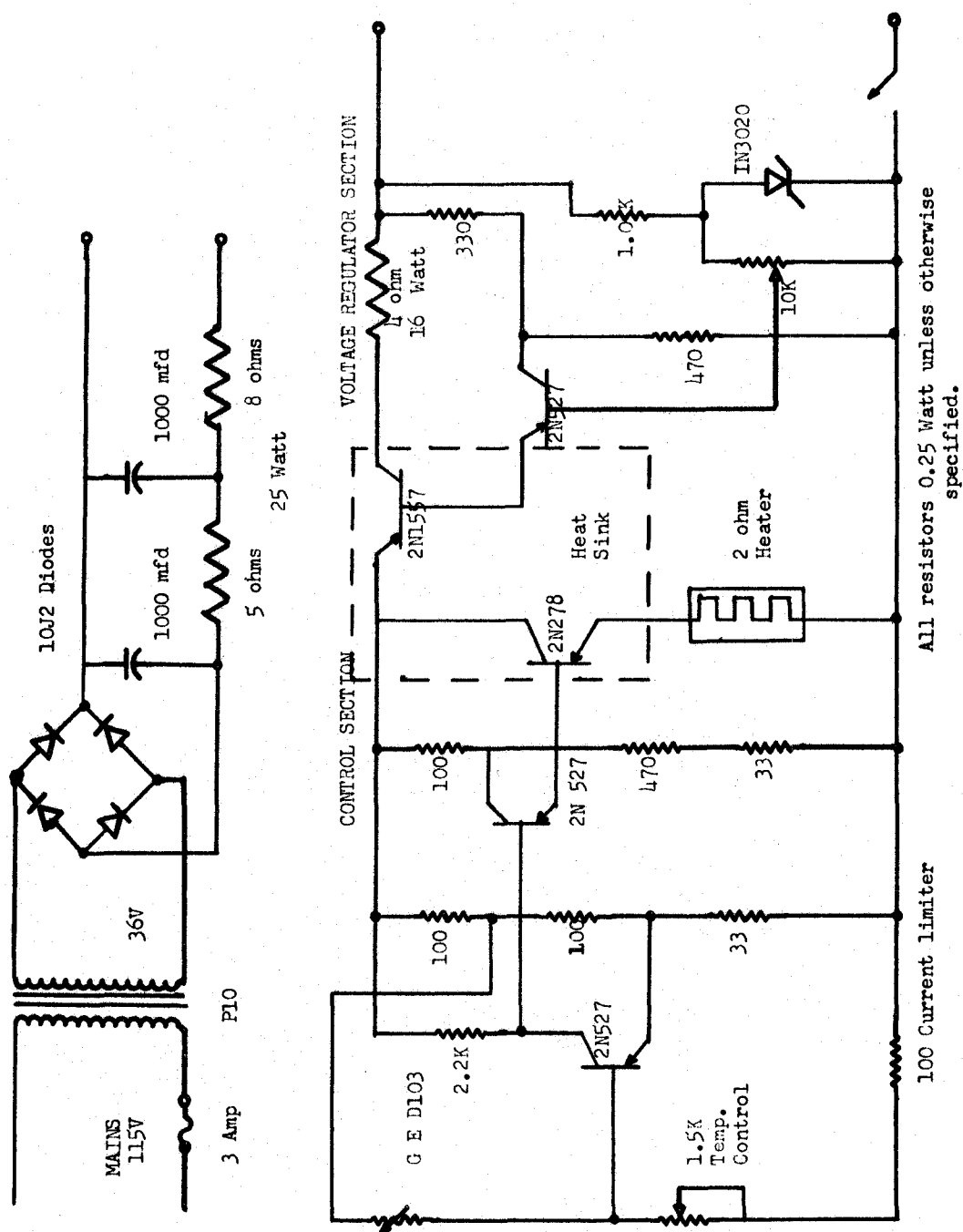


figure (4) The Heater Control Circuit

potentiometer in the screen grid circuit. With the circuit elements shown, the oscillator operates at 55mcs delivering a plate current of 300ma at 325V.

The lamp has been observed to operate in at least four modes. Only two of these occur frequently, and of these only one mode is of any use for the generation of resonance radiation. The useful mode is a skin discharge, where most of the light comes from the vapour in a thin layer close to the wall of the lamp. Only this discharge is characterized by dielectric heating of the lamp and emission of D lines. If the coil is properly tuned with the aid of a ceramic padder capacitor, this discharge can be produced with a plate current of 280ma at 325V and a total screen current of 15 - 20ma.

If the plate current is decreased to about 240ma, a discontinuous drop in current occurs as the plasma shifts to the axis of the lamp. Observation of fluorescent light from a sample of potassium vapour irradiated by the lamp during such a mode shift showed a complete cessation of fluorescence which indicates almost total self reversal in the light emitted in this type of discharge. The visual light intensity is virtually unchanged during this process.

The intensity of the light from the RF source depends critically on the density of the potassium vapour as does the degree of broadening and self-reversal in the D lines. The atomic density is controlled by the temperature of the reservoir of liquid potassium in the base of the lamp. A heater controller using a G.E.D103 thermistor as a sensing element determines the temperature of the lamp base and therefore the above listed lamp characteristics.

The heater itself was made of about 2 ohms of #28 Chromel A heating wire buried in the asbestos block supporting the lamp. Since the feedback path is essentially thermal, the thermistor must be placed properly with respect to the heater for critical damping. Otherwise the circuit may hunt or oscillate, causing intensity fluctuations. The circuit is inherently stable from the point of view of heat output. Voltage fluctuations do not affect it provided that they are not large enough to drive the voltage across the heater beyond the controlled range. If these surges are not a problem, the voltage regulator is not important except that it allows adjustment of the maximum current available to the heater and acts as a current limiter.

With the circuit elements shown in fig (4) the controller supplied currents from 0.35 amp to 1.45 amp to a 2.0 ohm load which corresponded to a maximum continuous power of 7.0 Watts. Immediately after switching on from a cold condition, the supply provided an uncontrolled current of 1.70 amp until discharge was established

Varying the temperature of the lamp produced sharp changes in line width and degree of self-reversal. This effect proved to be an advantage since, as the density of potassium vapour in the fluorescence cell increased, the sample accepted progressively broader lines. Increasing the width of the incident lines by means of lamp temperature helped to maintain a high intensity in the fluorescent light.

Two side effects of lamp operation also deserve mention. First as other workers have noted, (I. H. Brockman 1963) , hot potassium vapour attacks pyrex to form an opaque, brown, water-soluble deposit. This deposit interferes with lamp operation. However, the effect was

found to be reversible upon increasing the lamp temperature. Operating the lamp at plate currents in excess of 310 ma tends to keep it relatively free of these deposits. (A. G. A. Rae 1963)

Secondly, at all operating temperatures, the color of the RF discharge is yellow, characteristic not of potassium but of sodium. Neilsen and Wright (1930) have found from spectroscopic observations that this coloration is due to sodium impurities and partly to the enhancement of certain yellow argon lines at temperatures above 250° C.

## 2 The Monochromator.

A Baush & Lomb grating monochromator was used for the resolution of the potassium D lines in the incident light. This instrument, which has a focal length of 500 mm, a dispersion of 16 Å/mm and an aperture of  $f/4.4$ , contains a 1200 line/mm grating blazed at 7500 Å. With slit widths of 1.50 mm, a spectral purity of one part in 2000 was obtained. Measurements made at several slit widths indicated that the transmitted intensity varied linearly with slit width. The value of 1.50 mm was chosen to insure optimum spectral purity consistent with adequate intensity.

## 3 The Fluorescence Cell and the Furnace.

The construction of the fluorescence cell is shown in fig (5). The end and side windows were made of pyrex filter plate about 1 mm thick. The side window was set into the cell as close as possible to the front window to reduce absorption of incident radiation before it could reach the region under observation. The side arm, with a constriction about 10 cm from the cell, was made of standard 10 mm

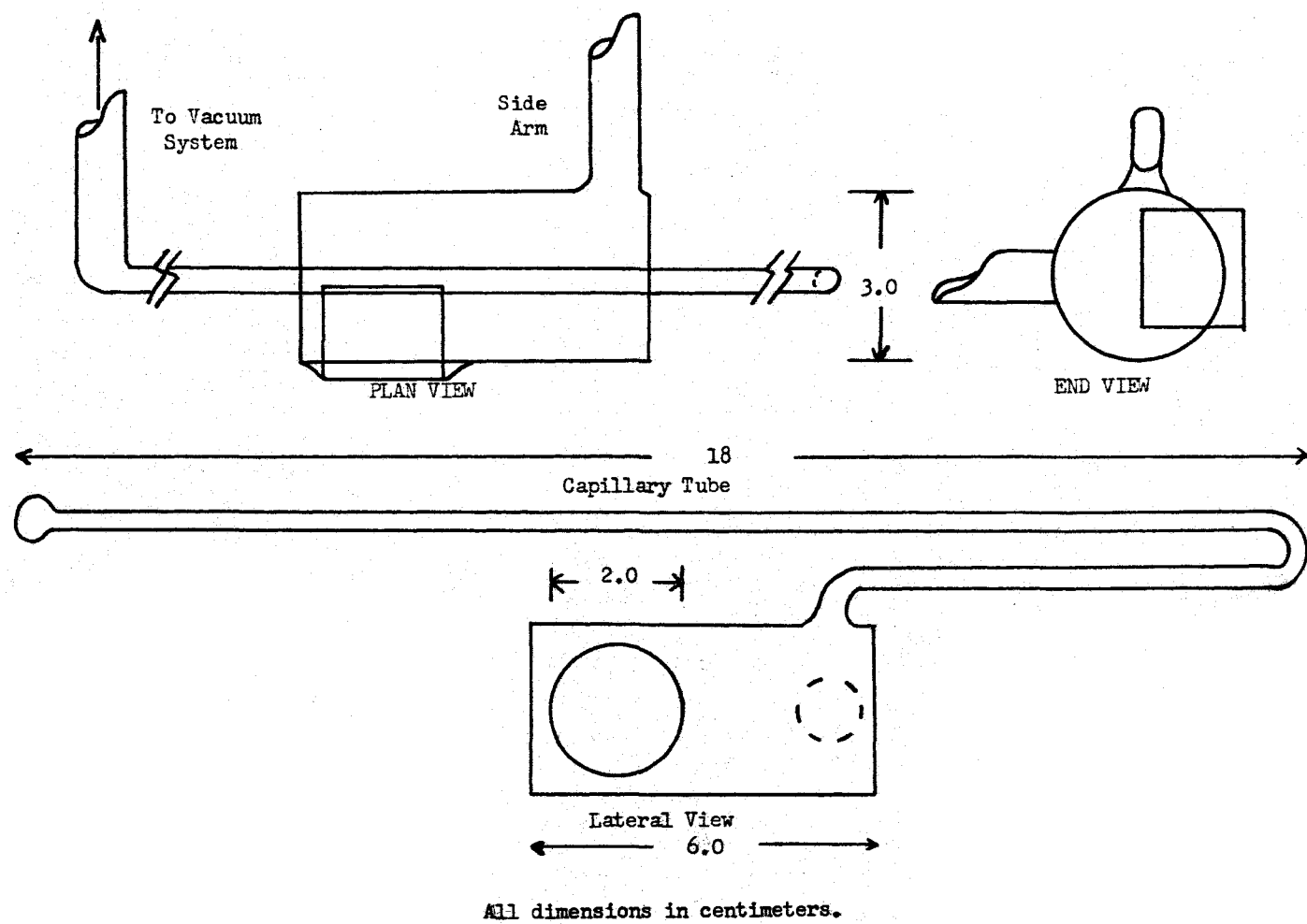


figure (5) Detail of the Fluorescence Cell

pyrex tubing. Both the side arm and capillary tube were connected to the vacuum and filling system at the beginning of each experiment.

Before connecting the side arm to the vacuum system, a small pyrex capsule, containing about 0.5 gm of potassium together with a steel breaker in a pyrex tube, was placed in it. The breaker, moved by means of a magnet, served to crack the thin-walled capsule to free the potassium, once a vacuum of  $2 \times 10^{-6}$  Torr or better obtained in the cell. The potassium in these capsules was 99.0% pure and was supplied by A.D. Mackay Inc., New York. It was vacuum distilled four times through a series of pyrex bulbs and into the capsules, which were sealed off under vacuum.

It has been found that the reaction of Potassium with the pyrex is enhanced by trace amounts of the mineral oil in which the potassium is stored. In the presence of oil, the glass of the fluorescence vessel may be deeply etched at relatively low temperatures ( $150^{\circ}\text{C}$ ). Because of this, it is desirable to wash the potassium in toluene or benzene before distilling it to remove all traces of oil. If the sample is clean, it may be maintained at  $200^{\circ}\text{C}$  for 10 hours or more before browning becomes noticeable.

An alkali resistant coating (Corning K - Coat), consisting of an aqueous solution of potassium fluoride dihydrate and boracic acid, was used in an attempt to eliminate browning altogether. Although this treatment does seem to limit the browning, it is extremely difficult to apply, is useless above  $300^{\circ}\text{C}$ , and may be used only once per cell. Its usefulness is offset by the difficulties it incurs.

The oven required to control the density of potassium vapour in the fluorescence cell was constructed in two sections, the main and the



side oven, as shown in figs (6) and (7). The main oven is a rectangular transite box divided into three sections. The two smaller sections at each end, filled with about 3 cm of asbestos insulation, provide space for power terminals and heating wire connections as well as thermal insulation of the entrance and exit windows.

All three central transite dividers are split horizontally. The top halves are bolted to the lid of the oven while the bottom halves are integral parts of the oven structure. This arrangement facilitates the insertion and removal of fluorescence cells. Both halves of the oven are provided with 32 ohms of #26 Chromel A heating wire strung in two banks of seven lengths along the axis of each section.

The entrance and exit windows are fitted with aluminum shutters and cover plates to minimize reflection, and the inside of the oven is coated with "Aquadag", an aqueous colloidal dispersion of graphite.

The fluorescence cell was clamped into a recess in the central cross - member by means of an aluminum strap. The side - arm extended through a hole in the back wall of the main oven into the side oven.

The side oven is constructed of two coaxial brass tubes separated by two annular transite pieces. The space between the tubes is filled with asbestos wool. The smaller tube projects 1.5 cm beyond the transite piece at one end of the oven and fits snugly into the hole in the main oven through which passes the side arm of the cell.

The side oven heater consists of a coil of about 20 ohms of #26 Chromel A heating wire which is wound on the insulated central tube and extends well into the wall of the oven. Such an arrangement ensures that a cold spot does not occur between the ovens and that a

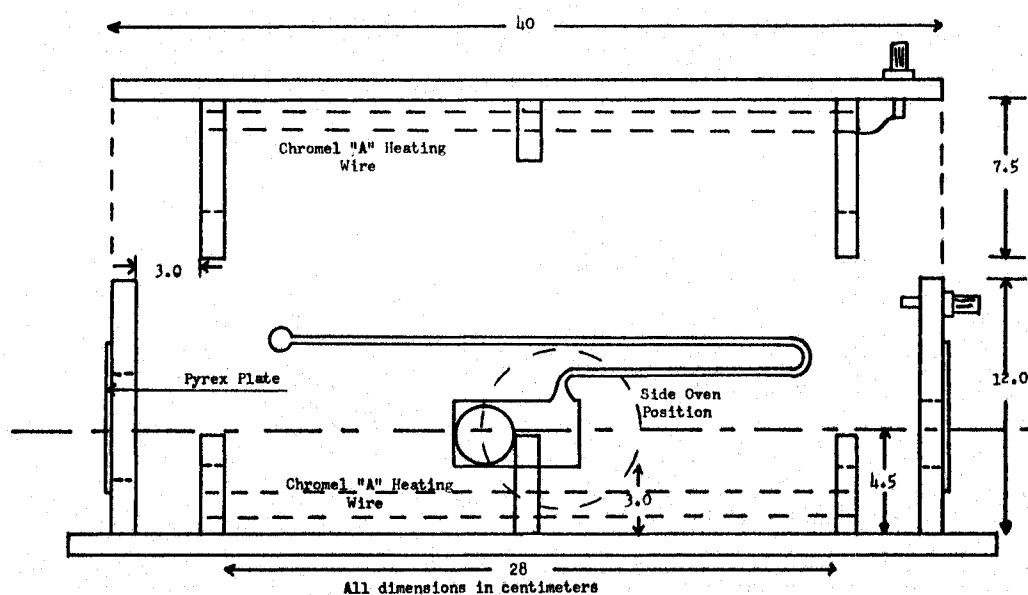


figure (6) Detail of the Oven Construction - Lateral View

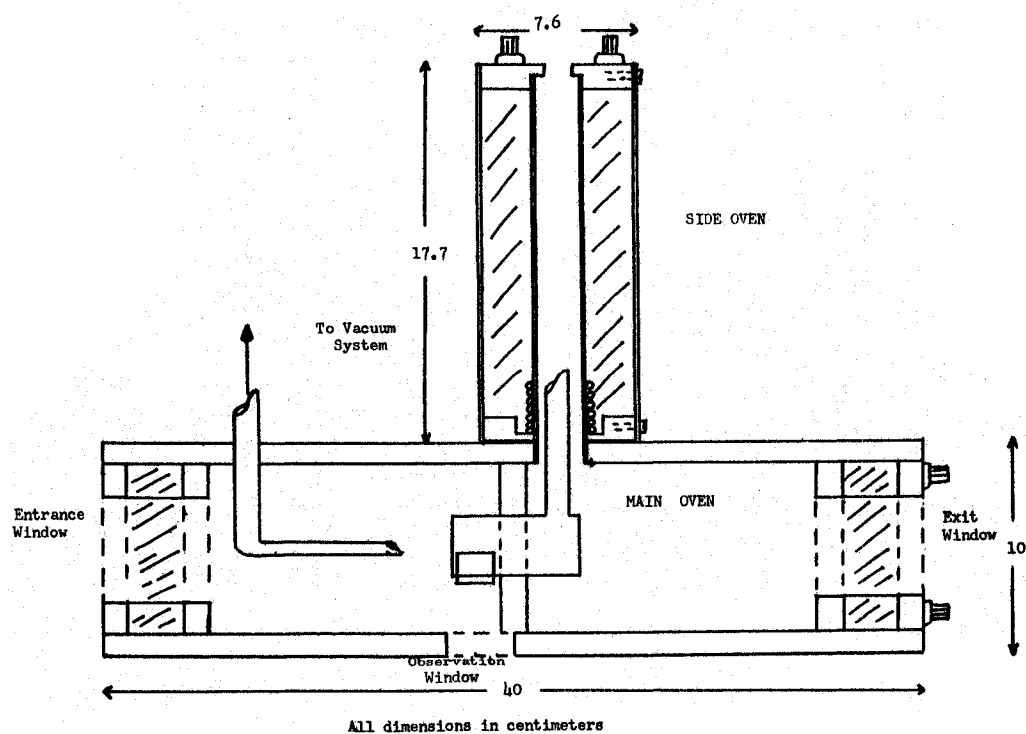


figure (7) Detail of the Oven Construction - Plan View

linear temperature gradient is established along the length of the side oven. This means that the end of the side arm, wherever it may be cut, is the coolest spot in the system. The temperature of the side arm, which is measured with a thermocouple, controls the vapour pressure of the potassium and prevents condensation on the cell windows.

Chromel - Alumel thermocouples were cemented with an asbestos paste to the cell near the front window and to the end of the side arm. The emf of the thermocouples, checked against an NRC - calibrated platinum - platinum rhodium thermocouple, was read with a Leeds and Northrup millivolt potentiometer (Cat. No. 8686). The temperature of the side oven so determined, was used in the calculation of the potassium vapour pressure by means of the empirical formula evolved by Ditchburn & Gilmour (1941) :

$$\log_{10} P(\text{Torr}) = - \frac{4552}{T} - 0.5 \log_{10} T + 8.793, \quad (25)$$

where T is in degrees Kelvin.

This formula appears to be much more accurate in approximating experimental results than that of Killian (1926). Even so, the probable error in pressure over the experimental range of temperatures is about 20%, which represents the greatest single source of experimental error.

The temperature of the main oven is not at all critical, provided that it is sufficiently above the side oven temperature to prevent condensation of potassium in the cell.

These ovens have the advantages of small size, low thermal capacity, and low power requirements. Temperatures are quickly changed and may be held to within  $0.25^{\circ}\text{C}$  without control or reproduced from calibration curves to within  $1.0^{\circ}\text{C}$ . The heating proceeds to a large

extent by radiation; coating the cell with " Aquadag " cuts off radiation to the inset side window, dropping its temperature by  $50^{\circ}\text{K}$  or more. The power requirements are 150 watts for the main oven and 40 watts for the side oven, to maintain a temperature of  $300^{\circ}\text{C}$ . Current is supplied independently to the two ovens by means of Variac auto-transformers which draw power from a Sorensen Isotran model MVR H 1000 voltage stabilizer.

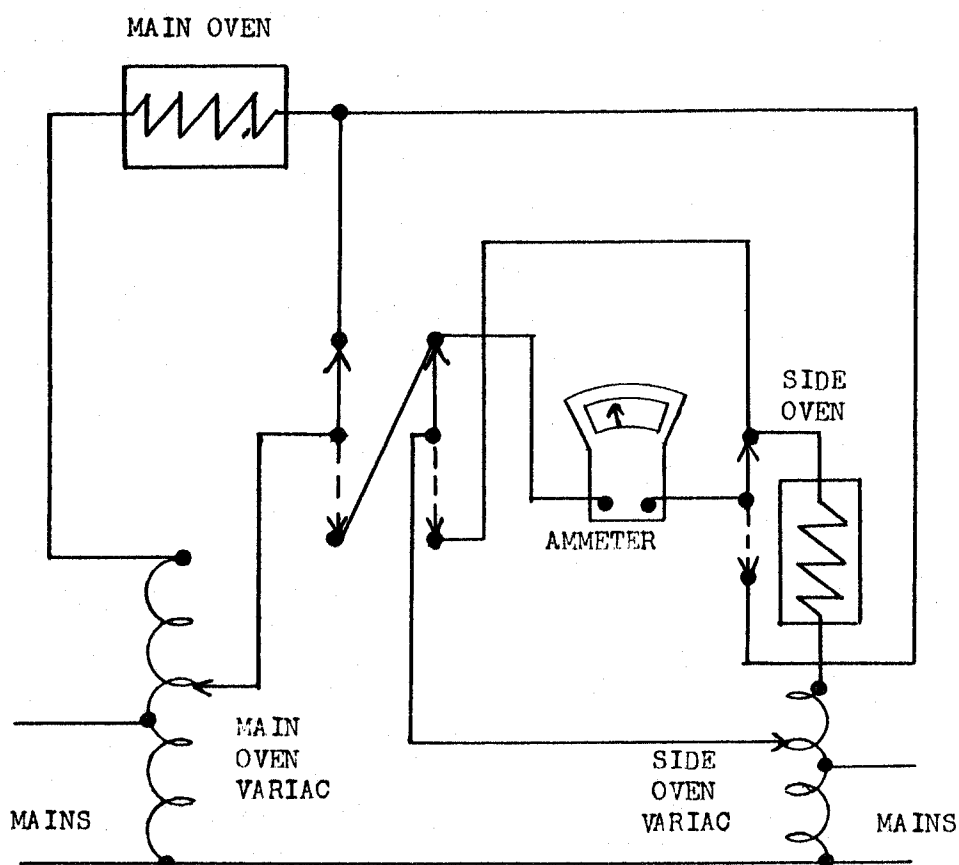


figure (8) Wiring of Oven Circuits

#### 4 The Evacuating and Filling System.

The glass system employed to evacuate the fluorescence cell and to admit to it controlled pressures of inert gases is shown in fig. (9). The high vacuum was produced by an Edwards Speedivac High Vacuum Pump Model 18050B fitted with a 2A non-return valve and a CEC MCF60 Oil Diffusion Pump filled with Dow Corning 704 Silicone pumping fluid. The diffusion pump was protected from cooling water failure by a Flowtrol type FSM - 1.

Pressure in the system was measured by means of a CEC Ionization Vacuum Gauge, Type GIC - 110, with a VG - 1A gauge head (in the range  $10^{-3}$  to  $10^{-8}$  Torr) and by an IKB Autovac Gauge Type 3294B with a Pirani gauge head (in the range  $10^{-3}$  to  $10^2$  Torr). For higher pressure a mercury manometer was used, and an oil manometer with silicone fluid (1.066gm/ml) was used between about 5 and 30 Torr, where the probable error in the Autovac gauge and mercury manometer is very large.

A Balzers micrometric needle valve Type VN-8 was installed to admit inert gases at controlled rates. The valve controls very well the rate of gas admittance but has the disadvantage, that it cannot be completely closed (Lower limit  $1 \times 10^{-5}$  Torr litre / sec ). This feature makes it necessary to isolate the valve after admitting a certain amount of gas at low pressures, or the pressure will rise constantly.

The stopcocks F and H connect the capillary tube and side arm of the cell, respectively, to the system. After evacuation and the introduction of a sample of metal, the line to H is disconnected by sealing off the side arm of the fluorescence tube. The volume of that

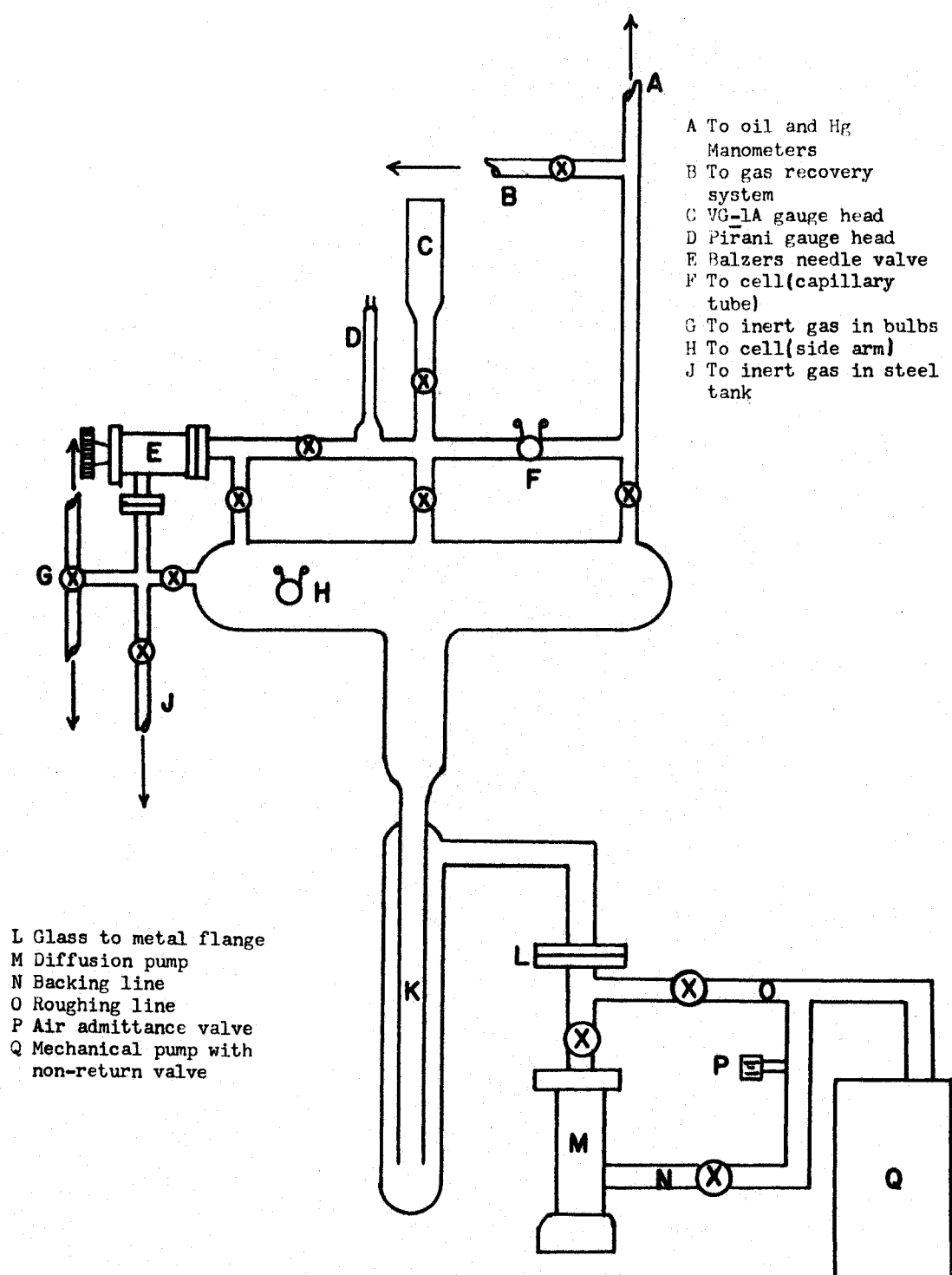


figure (9) The Vacuum and Filling System

part of the system, which must contain inert gas, is small (0.2 litre) to conserve the gases used.

The lowest pressure obtainable, with liquid air in the cold trap, was  $4 \times 10^{-7}$  Torr. However, during an actual experimental run  $1 \times 10^{-6}$  Torr was considered adequate.

## 5 The Recording Spectrometer.

The spectrometer is a modified version of the Perkin - Elmer Model 112 instrument in which the prism has been replaced by a Bausch & Lomb plane replica grating with 1200 grooves / mm and blazed at  $7500\text{\AA}$ . The instrument has a reciprocal dispersion of  $13\text{\AA}/\text{mm}$  and an aperture of  $f/4$ .

An external detection system was fitted to the spectrometer consisting of a multiplier phototube housed in a cryostat as described by Krause and Neville (1963). The phototube is a 16 - stage ITT FW 118 employing an S-1 (Ag-O-Cs) photocathode 3mm in diameter with a peak sensitivity of 0.0024 amperes per watt at  $8000\text{\AA}$ . The phototube output is fed into a Victoreen Electrometer amplifier Model VTE - 2 and then to a Daystrom Weston strip chart recorder.

The entrance and exit slit widths of the spectrometer were maintained at 0.80 mm. This setting gives the maximum intensity of transmitted light consistent with adequate resolution of the potassium resonance doublet.

## B The Optical Line Up.

The light source was placed about 3 cm from the entrance slit of the monochromator in order to fill the optics of the instrument with light. An  $f/1.0$  lens of focal length 5.5 cm was located 64.3 cm from the parabolic mirror in the monochromator. An  $f/2.9$  lens of focal

length 26.0 cm, 62.5 cm beyond the first lens, formed an image of the exit slit of the monochromator in the fluorescence cell, in front of the side window. The window and image were situated 48.5 cm from the second lens. The image so formed was 10 mm in height and 1.0 mm wide. The system was so designed as to form an image of the parabolic mirror 7.8 mm square and 47.0 cm from the second lens. In the course of time, the surface - silvered mirror collected a small amount of dust which was difficult to remove without marring the silver layer. The layer of dust scatters light, making the illuminated portion of the mirror a weak second object for the lens system. If this source of light is not properly focused, or if the mirror is not scrupulously clean, the light so scattered may be reflected in the cell and be detected by the spectrometer as stray light of the incident wavelength.

Very little light is lost in this system apart from surface reflections from the lenses so that a high intensity image is formed in the fluorescence cell. The length of the cone of light entering the oven and its small angle of divergence ( $\sim 11^\circ$ ) ensure that there will be no reflection off the walls of the cell when the second lens is properly adjusted.

The monochromator and the lenses were placed on a heavy table made of welded two inch angle iron. The lenses were mounted in carriages on an optical bench bolted securely to the table. The lens carriages were fitted with knurled screws to permit vertical and lateral adjustment of the lens positions.

The position of  $L_2$ , an  $f/1.11$  lens of focal length 10 cm, situated between the oven and the spectrometer, is variable. It was adjusted at the beginning of each experiment for maximum intensity,



since the position of the fluorescent region in the cell depends to some extent on cell geometry. However, a position 23 cm from the spectrometer and 19 cm from the cell window is fairly typical.

#### IV RESULTS AND DISCUSSION

##### Sensitized Fluorescence in Potassium Vapour.

At the beginning of an experimental run, the fluorescence cell was thoroughly outgassed by heating to  $250^{\circ}\text{C}$  while pumping through both the capillary tube and the side arm. When a pressure of  $2 \times 10^{-6}$  Torr, or less, was reached, the pyrex capsule containing the potassium was broken with the steel breaker by means of a small permanent magnet. The potassium was very slowly distilled through the constriction into the side arm of the fluorescence cell until about half of the potassium remained in the capsule. This procedure helps to eliminate low vapour pressure impurities, mainly sodium, and leads to more reproducible experimental results than would otherwise be obtained. The side arm was sealed off under vacuum and disconnected from the vacuum system at a point 10 to 14 cm from the body of the cell. The remainder of the side arm containing the capsule, breaker, and residual potassium, was then removed from the vacuum system. Finally, the thermocouple was attached to the end of the side arm and the side oven slid into place.

The lens  $L_2$  (fig 1) was then adjusted, with the ovens at room temperature, so that the image of the monochromator exit slit was placed as close as possible to the side window without producing reflections. The position of the image depends primarily on cell geometry and varies slightly from cell to cell. The lens between the oven and the spectrometer was adjusted for maximum light intensity with the ovens at about  $60^{\circ}\text{C}$  so that some fluorescent light was available. The ovens were brought up to temperature, the light source

switched on, and the power to the photomultiplier (1.8 KV) and electrometer turned on. The equipment was allowed to stabilize for at least one hour before any readings were taken.

After the equipment had reached stable operating conditions, one of the potassium D lines was made incident on the fluorescence cell. The fluorescent spectrum was scanned twice. The other D line was then made incident and again the spectrometer made two scans through the fluorescent spectrum. This procedure was followed until four scans had been made with each of the D lines incident. The intensity ratios calculated from the strip chart records of these scans of the spectrum were then averaged to yield values of  $\eta_1$  and  $\eta_2$  for a given temperature. If the ratio showed considerable scatter due to low intensity, then six or seven scans would be made with each line incident to obtain a better average. The ratios were then corrected for the effects of reflection and spectral impurity.

Table 1 gives the experimental values for  $\eta_1 = \frac{I_1}{I_2}$  and  $\eta_2 = \frac{I_2}{I_1}$ , where  $I_1$  is the intensity of the 7699 Å component and  $I_2$  is the intensity of the 7665 Å component. In each case, the intensity of that component of the fluorescent spectrum which is present in the exciting beam is given as the denominator. These ratios were obtained by using three different samples of potassium in two fluorescence cells. Reproducibility was at all times the criterion for retention of any ratio.

The data from Table 1 were plotted linearly against potassium vapour pressure as shown in figures (10) and (11). Representative points obtained by Thangaraj (1948) and Hoffmann and Seiwert (1961) are presented for comparison. The values of  $\eta_2$  found in this

TABLE 1  
Intensity Ratios in Sensitized Fluorescence Induced  
by Potassium - Potassium Collisions.

Temp. °K	Pressure (Torr)	Excitation with 7665Å ( $I_2$ )	Excitation with 7699Å ( $I_1$ )	Run No.
		$\eta_1 = I_1/I_2$	$\eta_2 = I_2/I_1$	
364	$1.0 \times 10^{-5}$	0.00195	0.00185	5
369	$1.5 \times 10^{-5}$	0.00970	0.00772	4
370	$1.6 \times 10^{-5}$	0.00298	0.00198	1
376	$2.63 \times 10^{-5}$	0.00687	0.00561	1
378	$2.8 \times 10^{-5}$	0.00653	0.00471	5
379	$3.1 \times 10^{-5}$	0.01305	0.01361	4
387	$5.3 \times 10^{-5}$	0.01852	0.01530	1
389	$6.2 \times 10^{-5}$	0.0318	0.0205	4
400	$1.3 \times 10^{-4}$	0.0350	0.0316	1
400	$1.3 \times 10^{-4}$	0.0390	0.0444	4
406	$1.9 \times 10^{-4}$	0.0521	0.0422	5
409	$2.3 \times 10^{-4}$	0.0540	0.0453	1
411	$2.6 \times 10^{-4}$	0.0645	0.0791	4
420	$4.4 \times 10^{-4}$	0.1233	0.1070	5
421	$4.7 \times 10^{-4}$	0.1231	0.1168	1
422	$5.0 \times 10^{-4}$	0.104	0.212	4
432	$8.5 \times 10^{-4}$	0.202	0.200	1
437	$1.15 \times 10^{-3}$	0.238	0.264	5
438	$1.2 \times 10^{-3}$	0.138	0.296	4
441	$1.4 \times 10^{-3}$	0.237	0.250	1
448	$2.05 \times 10^{-3}$	0.289	0.430	5

TABLE 1 (continued)

Temp. °K	Pressure (Torr)	Excitation with 7665Å ( $I_2$ )	Excitation with 7699Å ( $I_1$ )	Run No.
		$\eta_1 = I_1/I_2$	$\eta_2 = I_2/I_1$	
450	$2.25 \times 10^{-3}$	0.263	0.318	1
457	$3.2 \times 10^{-3}$	0.316	0.646	5
471	$6.25 \times 10^{-3}$	0.371	0.728	1
471	$6.25 \times 10^{-3}$	0.404	0.822	5
485	$1.15 \times 10^{-2}$	0.458	0.943	4
494	$1.7 \times 10^{-2}$	0.499	1.031	5
497	$1.92 \times 10^{-2}$	0.508	1.005	4
506	$2.8 \times 10^{-2}$	0.614	1.173	5
507	$2.9 \times 10^{-2}$	0.572	- - -	4
517	$4.2 \times 10^{-2}$	0.628	- - -	4
518	$4.3 \times 10^{-2}$	0.654	1.240	5
529	$6.6 \times 10^{-2}$	0.690	1.311	5
533	$7.7 \times 10^{-2}$	0.650	1.310	5
539	$9.4 \times 10^{-2}$	0.685	- - -	4
540	$9.6 \times 10^{-2}$	0.679	1.381	5
546	$1.2 \times 10^{-1}$	0.655	1.333	4
550	$1.38 \times 10^{-1}$	0.626	1.312	5

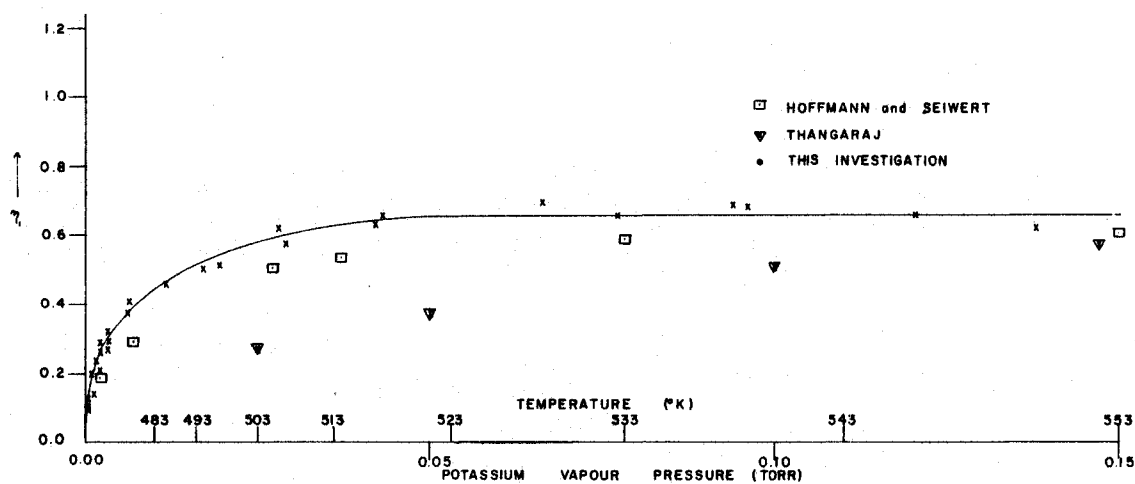


figure (10) The Variation of  $\eta_1 = I_1/I_2$  With Potassium Vapour Pressure

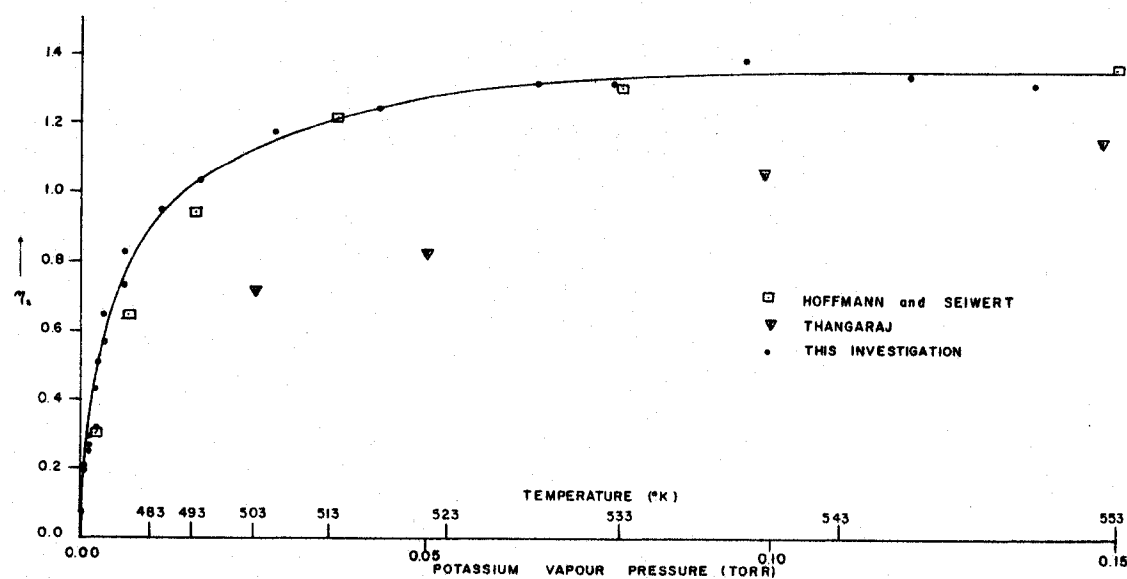


figure (11) The Variation of  $\eta_2 = I_2/I_1$  With Potassium Vapour Pressure

investigation agree very well with those of Hoffmann and Seiwert, while for  $\gamma_1$  the results of this investigation at high pressure are about 6% higher than those of Hoffmann and Seiwert.

The values of both ratios found by Thangaraj are very much lower at all pressures. This is to be expected if the theoretical expectations set out in section II are correct, since Thangaraj worked under conditions in which radiation diffusion must have been a dominant factor.

As the vapour density of potassium is increased, the ratio of the populations of the two excited states should approach the ratio of their statistical weights. The  $^2P_{3/2}$  level has a 4 - fold degeneracy and therefore a statistical weight of 4. Similarly, the statistical weight of the  $^2P_{1/2}$  level is 2. It is to be expected, then, that as the vapour density of potassium increases,  $\gamma_1$  and  $\gamma_2$  should approach the values of 0.5 and 2.0 respectively. In fact,  $\gamma_1$  and  $\gamma_2$  reach constant values of 0.655 and 1.35, respectively. The same effect was observed by Hoffmann and Seiwert. This deviation from predicted values is most readily explained by the fact that the absorption coefficient of the 7665Å component is twice that of the 7699Å component. This difference in absorption would tend to increase  $\gamma_1$  and decrease  $\gamma_2$  as radiation diffusion becomes more and more significant.

The values of the intensity ratios are plotted semi-logarithmically against potassium vapour pressure in figure (12). The semi-log plot is made necessary by the fact that potassium vapour pressure was varied by five orders of magnitude in these experiments. The low-pressure detail is lost in a linear plot of the whole experimental range of vapour pressures.

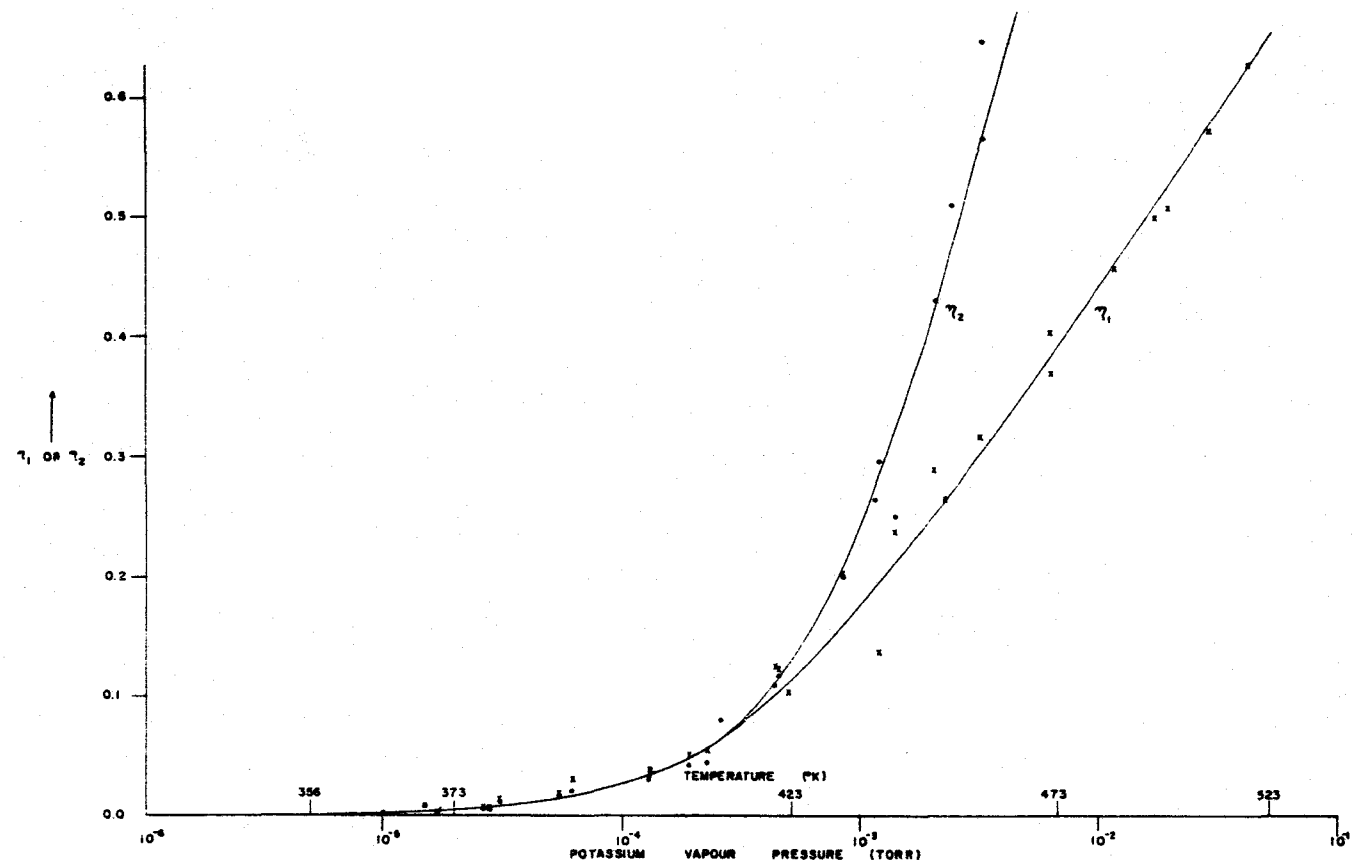


figure (12) A Semi - Logarithmic Plot of  $\gamma_1 = I_1/I_2$  and  $\gamma_2 = I_2/I_1$   
Against Potassium Vapour Pressure



The region of the curves from  $1 \times 10^{-5}$  to about  $7 \times 10^{-4}$  Torr and from  $3 \times 10^{-3}$  to  $1.5 \times 10^{-1}$  Torr was reproducible in all three experimental runs. However, the region between  $7 \times 10^{-4}$  and  $3 \times 10^{-3}$  Torr was decidedly non-reproducible except in the case where the distance of the slit image in the cell to the side window was exactly duplicated in two runs. As Hoffmann and Seiwert (1961) have found, the values of  $\eta_1$  and  $\eta_2$  in this pressure range depend critically on the distance between the fluorescent spot and the side window. This would seem to indicate that this pressure range marks the onset of radiation diffusion.

In all cases, within a given run, when the cell geometry was unaltered, both intensity ratios fell on smooth curves. The values indicated in fig (12) in the range  $7 \times 10^{-4}$  to  $3 \times 10^{-3}$  Torr must therefore be taken as representative rather than quantitative. Many more points than those shown were actually taken in this region, but only the most reproducible were used to avoid confusion. This geometry dependence is not troublesome, since it occurs well above the pressure range in which the experimental determination of cross sections were to be made. The values of  $\eta_1$  and  $\eta_2$  obtained in the absence of radiation imprisonment are the most useful.

It is significant that at  $3 \times 10^{-4}$  Torr the curves for  $\eta_1$  and  $\eta_2$  merge; the two ratios are identical below this pressure. For pressures below  $3 \times 10^{-4}$  Torr, no comparison with previous work can be made, since fluorescence at these low vapour densities has not been previously observed. The merging of the intensity ratios implies that the collision numbers and cross sections for the upward and downward transitions become equal. This effect might be explained by assuming that the component of the total angular momentum of the colliding

system is conserved along the collision axis. More will be said of this in the second half of this section. Below  $3 \times 10^{-4}$  Torr there should be no effects due to radiation imprisonment and the intensity ratios observed at these pressures should yield true cross sections for inelastic collisions in the absence of radiation imprisonment.

Figure (13) is a linear plot of intensity ratios, collision numbers, and cross sections against potassium vapour pressure in the region where radiation diffusion is not significant. The straight line drawn through the points representing values of  $\eta_1$  and  $\eta_2$  is a good estimate of the mean positions of the experimental points. This line is the same as the one which appears on the semi-logarithmic plot of  $\eta_1$  and  $\eta_2$ .

From the straight line curve for  $\eta_1$  and  $\eta_2$ , values were taken and used with the aid of equation (20) to calculate  $Z_1$  and  $Z_2$ , which are identical in this region. These values are given in Table 2 and, when they are plotted against potassium vapour pressure, a straight line results. This linear variation with potassium vapour pressure is very significant and indicates that these results are likely to be correct.

The accuracy with which  $\eta_1$  or  $\eta_2$  can be experimentally measured depends upon the magnitude of the ratios. The sensitized fluorescence produced by collisions is of very low intensity and the signal to noise ratio of the photomultiplier system becomes the determining factor in experimental precision as the vapour pressure decreases to very low values. For example, at  $1 \times 10^{-5}$  Torr, single values of  $\eta_1$  and  $\eta_2$  have a probable error of about 30%. Taking values from the straight line through the points representing  $\eta_1$  and  $\eta_2$  decreases this experimental error to some extent. Even so, if cross sections are calculated

TABLE 2

Collision Numbers in Sensitized Fluorescence Induced by  
Potassium - Potassium Collisions

Pressure (Torr)	$\eta_1 = I_1/I_2$	$\eta_2 = I_2/I_1$	${}^2P_{1/2} \xrightarrow{Z_1} {}^2P_{3/2}$ Coll/atom/sec	${}^2P_{3/2} \xrightarrow{Z_2} {}^2P_{1/2}$ Coll/atom/sec
$2.0 \times 10^{-5}$	0.005	0.005	$1.94 \times 10^5$	$1.94 \times 10^5$
$3.6 \times 10^{-5}$	0.009	0.009	$3.49 \times 10^5$	$3.49 \times 10^5$
$5.0 \times 10^{-5}$	0.013	0.013	$5.07 \times 10^5$	$5.07 \times 10^5$
$7.0 \times 10^{-5}$	0.018	0.018	$7.04 \times 10^5$	$7.04 \times 10^5$
$1.0 \times 10^{-4}$	0.026	0.026	$1.03 \times 10^6$	$1.03 \times 10^6$
$1.2 \times 10^{-4}$	0.031	0.031	$1.23 \times 10^6$	$1.23 \times 10^6$
$1.4 \times 10^{-4}$	0.036	0.036	$1.44 \times 10^6$	$1.44 \times 10^6$
$1.6 \times 10^{-4}$	0.042	0.042	$1.69 \times 10^6$	$1.69 \times 10^6$
$2.0 \times 10^{-4}$	0.052	0.052	$2.12 \times 10^6$	$2.12 \times 10^6$
$2.4 \times 10^{-4}$	0.062	0.062	$2.55 \times 10^6$	$2.55 \times 10^6$
$2.8 \times 10^{-4}$	0.073	0.073	$3.02 \times 10^6$	$3.02 \times 10^6$
$3.0 \times 10^{-4}$	0.078	0.078	$3.25 \times 10^6$	$3.25 \times 10^6$
$4.0 \times 10^{-4}$	0.093	0.099	$4.20 \times 10^6$	$3.97 \times 10^6$
$6.0 \times 10^{-4}$	0.126	0.144	$6.34 \times 10^6$	$5.56 \times 10^6$
$8.0 \times 10^{-4}$	0.153	0.195	$8.92 \times 10^6$	$7.25 \times 10^6$
$1.0 \times 10^{-3}$	0.176	0.240	$1.13 \times 10^7$	$8.77 \times 10^6$
$1.5 \times 10^{-3}$	0.218	0.338	$1.71 \times 10^7$	$1.21 \times 10^7$
$2.0 \times 10^{-3}$	0.249	0.413	$2.21 \times 10^7$	$1.51 \times 10^7$
$3.0 \times 10^{-3}$	0.294	0.538	$3.18 \times 10^7$	$2.06 \times 10^7$
$5.0 \times 10^{-3}$	0.356	0.700	$4.85 \times 10^7$	$3.09 \times 10^7$

TABLE 2 (continued)

Pressure (Torr)	$\eta_1 = I_1/I_2$	$\eta_2 = I_2/I_1$	$\xrightarrow{Z_1} \text{ } ^2P_{1/2} \rightarrow ^2P_{3/2}$ Coll/atom/sec	$\xrightarrow{Z_2} \text{ } ^2P_{3/2} \rightarrow ^2P_{1/2}$ Coll/atom/sec
$7.0 \times 10^{-3}$	0.398	0.800	$6.31 \times 10^7$	$4.04 \times 10^7$
$8.5 \times 10^{-3}$	0.423	0.856	$7.35 \times 10^7$	$4.74 \times 10^7$
$1.0 \times 10^{-2}$	0.445	0.900	$8.35 \times 10^7$	$5.44 \times 10^7$
$1.2 \times 10^{-2}$	0.468	0.945	$9.55 \times 10^7$	$6.29 \times 10^7$
$1.3 \times 10^{-2}$	0.480	0.965	$1.02 \times 10^8$	$6.77 \times 10^7$
$2.0 \times 10^{-2}$	0.538	1.076	$1.51 \times 10^8$	$1.02 \times 10^8$
$3.0 \times 10^{-2}$	0.592	1.170	$2.33 \times 10^8$	$1.60 \times 10^8$
$4.0 \times 10^{-2}$	0.630	1.228	$3.39 \times 10^8$	$2.38 \times 10^8$
$5.0 \times 10^{-2}$	0.650	1.275	$4.74 \times 10^8$	$3.29 \times 10^8$
$6.0 \times 10^{-2}$	0.655	1.303	$5.68 \times 10^8$	$3.96 \times 10^8$
$7.0 \times 10^{-2}$	0.655	1.320	$6.24 \times 10^8$	$4.31 \times 10^8$
$8.0 \times 10^{-2}$	0.655	1.332	$6.63 \times 10^8$	$4.59 \times 10^8$
$9.0 \times 10^{-2}$	0.655	1.340	$6.99 \times 10^8$	$4.81 \times 10^8$
$9.5 \times 10^{-2}$	0.655	1.343	$7.15 \times 10^8$	$4.90 \times 10^8$
$1.0 \times 10^{-1}$	0.655	1.350	$7.40 \times 10^8$	$5.10 \times 10^8$

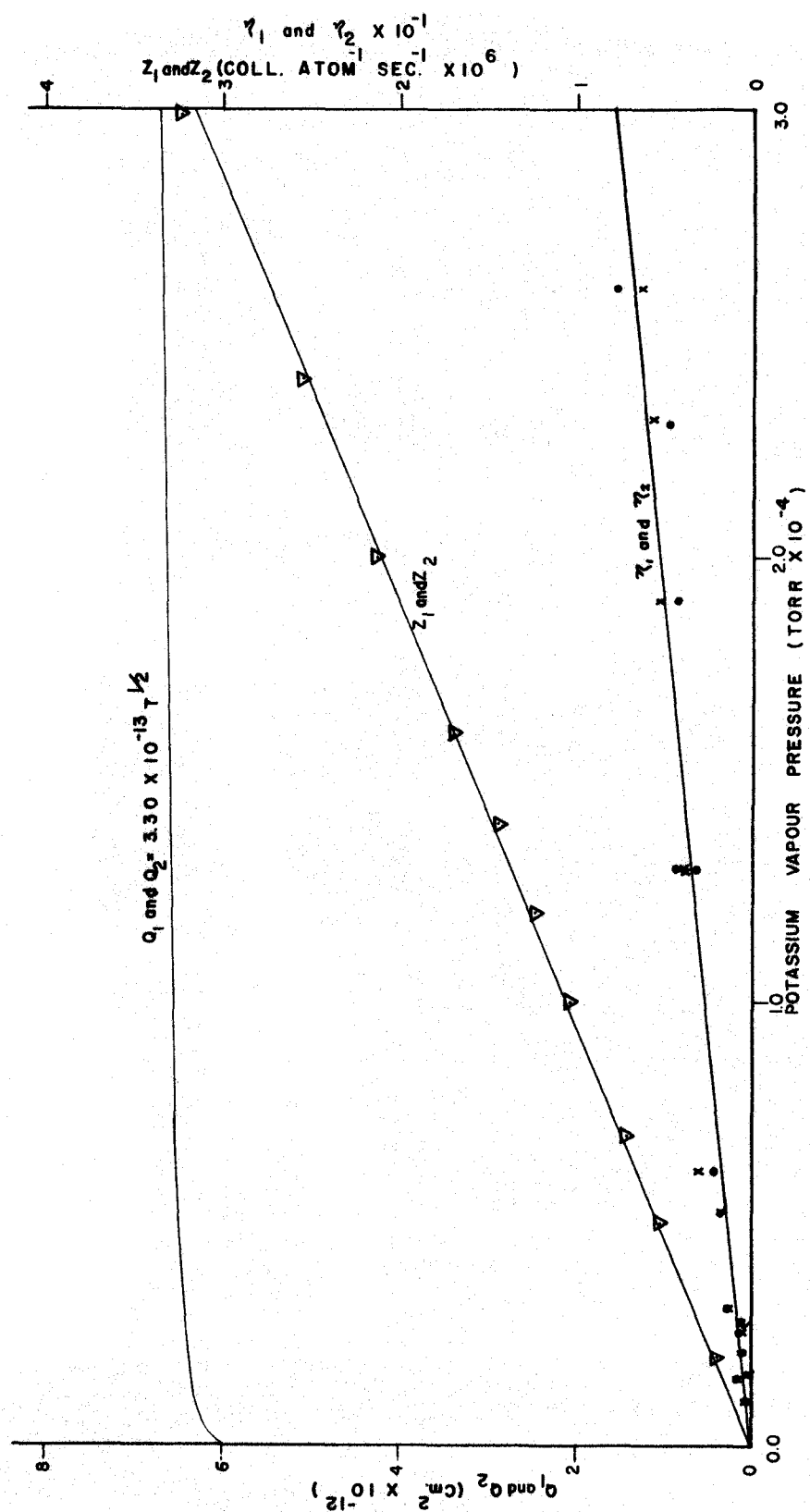


figure (13) The Variation of  $\eta$ ,  $Z$ , and  $Q$  With Potassium Vapour Pressures at Low Potassium Densities

point for point from values of the collision numbers at low potassium vapour pressures, the probable error will be very high because of the probable error of 20% in the vapour pressure as calculated from the absolute temperature.

Since the collision numbers in the absence of radiation imprisonment vary linearly with pressure, a means is provided whereby the errors involved in the measurement of the intensity ratios and in the calculation of the cross section can be largely eliminated. The cross section, as represented by equation (24), varies as the first derivative of the collision number with respect to pressure, except for the  $\sqrt{T}$  variation which is extremely slow over the diffusion - free pressure range. Since the collision number varies linearly with potassium vapour pressure, the first derivative, or slope, of this line is a constant, equal to  $1.05 \times 10^{10}$  collisions  $\text{atom}^{-1} \text{ sec}^{-1} \text{ Torr}^{-1}$ . Therefore the cross section depends only on  $\sqrt{T}$  in this region of potassium vapour pressures. The cross sections  $Q_1$  and  $Q_2$  are both given explicitly by

$$Q = 3.30\sqrt{T} \times 10^{-13} \text{ cm}^2.$$

Thus, the cross sections have been reduced to a function of the relative velocity only. At  $2.0 \times 10^{-4}$  Torr, this relationship gives

$$Q = 6.6 \times 10^{-12} \text{ cm}^2.$$

The results are compared below with those obtained by Thangaraj and Hoffmann and Seiwert.

Source	$Q_1 (\text{cm}^2)$	$Q_2 (\text{cm}^2)$
This investigation	$6.6 \times 10^{-12}$	$6.6 \times 10^{-12}$
Thangaraj (1948)	$3.3 \times 10^{-14}$	$1.65 \times 10^{-14}$
Hoffmann & Seiwert (1961)	$1.2 \times 10^{-14}$	$0.6 \times 10^{-14}$

The discrepancies indicated in the above comparison are due to

two factors. This investigation was carried out in the absence of radiation imprisonment. Since Thangaraj worked in the region of surface fluorescence, and Hoffmann and Seiwert obtained most of their data in the region of volume fluorescence, extensive theoretical compensation for the effects of radiation diffusion was necessary in both cases. Thangaraj used Milne's theory (1926) while Seiwert adapted Holstein's theory (1947) to his experimental conditions. Neither of these authors obtained experimental data under diffusion free conditions, so that their final values for  $Q_1$  and  $Q_2$  depended on theoretical assumptions about the effectiveness of radiation diffusion and the effects of the geometry of their experimental arrangements. In addition, both Thangaraj and Hoffmann and Seiwert were dependent upon an exact knowledge of the absolute density of the alkali vapours in their systems. Such an exact knowledge of vapour density was not necessary in this investigation, nor were any theoretical corrections required.

The error possible in values of  $Q$  calculated point - for - point from the collision numbers would be about 30%. This figure is based upon a probable error in vapour pressure of 20% as specified by Ditchburn and Gilmour (1941). The error in pressure is probably due to the error involved in the measurement of one of the constants in equation (25). This, in turn, is due to an inexact knowledge of the rate of change of the heat of vapourization of potassium as it affects the Clausius - Clapeyron equation. Thus, although the pressures determined with the aid of equation (25) may be above or below the "true" vapour pressure of potassium, the pressures will be consistent among themselves. If the cross sections are calculated point - for - point from values for the collision numbers, any probable error in

pressure will appear in the cross sections. However, the slope of the collision number curve is independent of the absolute pressure, provided that the pressures measured are consistent among themselves. Therefore, if such a linear variation occurs, the only error attributable to pressure appearing in the cross sections is due to the inaccuracy in absolute temperature measurement. This source of error was comparatively insignificant.

The largest error occurs in the measurement of specific values of  $\eta_1$  and  $\eta_2$  and it amounts to about 10% in the region of low radiation diffusion. In this region the 10% possible error in  $\eta$  appears directly in  $Z$  and  $Q$ .

As indicated in Section II, the variation of  $Z$  with pressure is accurately measureable only if diffusion is absent. Extrapolation of the linear region of the collision number curve to higher pressures should represent the true variation of the collision numbers unchanged by diffusion effects.

The experimental determinations of  $Z_1$  and  $Z_2$  at higher pressures, found in Table II, are plotted semi-logarithmically against potassium vapour pressure in fig (14). The extrapolation of the linear region of  $Z_1$  and  $Z_2$  is plotted in the same figure for comparison. As predicted in section II, the collision numbers at higher pressures fall below the values obtained by extrapolation.  $Z_2$  deviates from the extrapolated curve at about  $3 \times 10^{-4}$  Torr while  $Z_1$  follows the extrapolated curve to a vapour pressure of  $3 \times 10^{-3}$  Torr. The reason why  $Z_1$  follows the extrapolated curve to higher pressures than  $Z_2$  is due to the change in apparent lifetimes of the excited states. As proposed in section II, the lifetimes of both excited states will be artificially



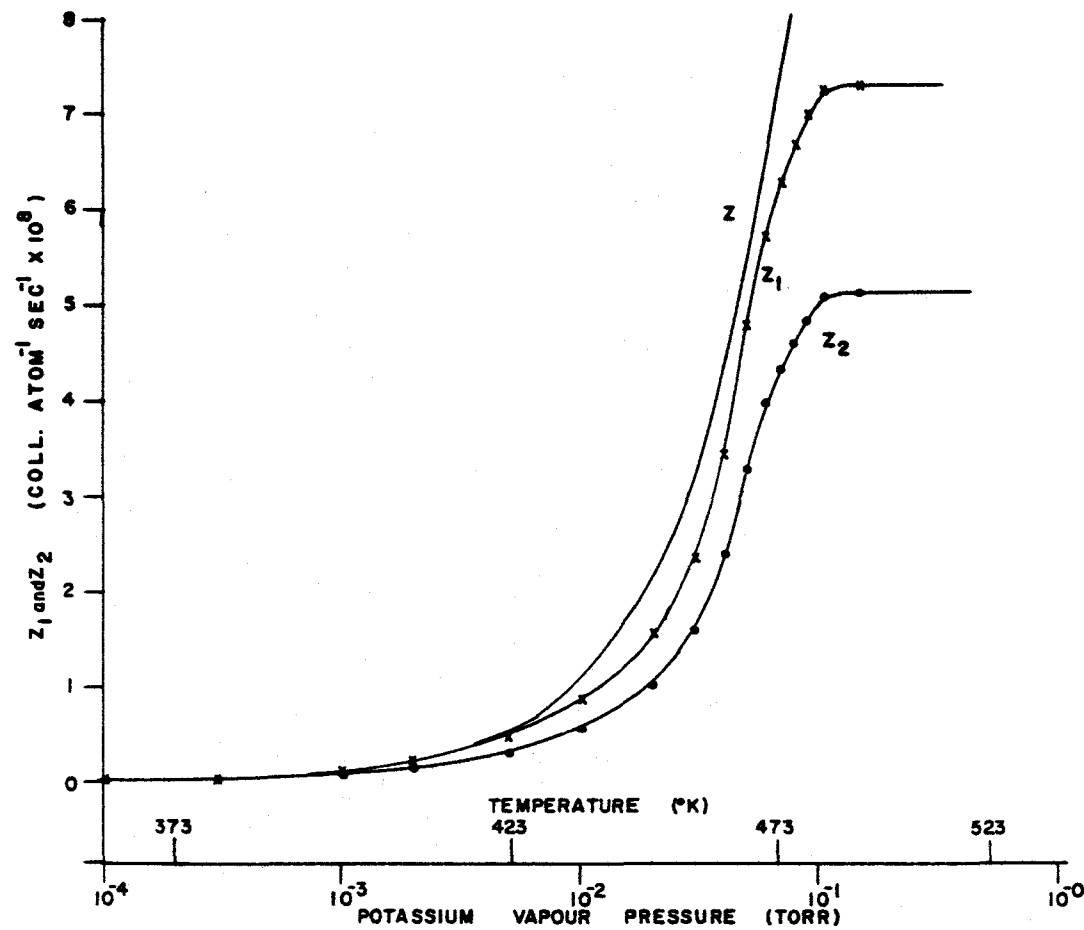


figure (114) A Semi - Logarithmic Plot of  $Z_1$  ( $^2P_{1/2} \rightarrow ^2P_{3/2}$ ) and  $Z_2$  ( $^2P_{3/2} \rightarrow ^2P_{1/2}$ ) Against Potassium Vapour Pressure  
 $Z$  is an Extrapolation of the Linear Region of the  $Z_1$  and  $Z_2$  Curves

lengthened. This manifests itself as a decrease in  $\eta_2$  and an increase in  $\eta_1$ . Since the absorption coefficient for the  $7665\text{\AA}$  component is twice that of the  $7699\text{\AA}$  component, the apparent lifetime of the  $2P_{3/2}$  state will increase more rapidly than that of the  $2P_{1/2}$  state. Therefore, the collision number  $Z_2$  should decrease more rapidly than  $Z_1$  with increasing vapour pressure.

Much the same argument holds true for  $Q_1$  and  $Q_2$  with increasing potassium vapour pressure. The cross sections drop below the extrapolated values at the same pressures as the corresponding collision numbers.

#### The Total Intensity of Fluorescence in Potassium Vapour.

The total fluorescent intensities ( $I_1 + I_2$ ) for both of the potassium D lines used in turn in the exciting beam are listed in Table 3 and plotted against the potassium vapour pressure in figure (15). These intensities were obtained using the radio frequency source previously described. The lamp was operated at a low temperature which caused the exciting lines to be quite narrow and little self reversed.

From  $3 \times 10^{-6}$  Torr to  $5 \times 10^{-5}$  Torr, the total intensity with the  $7699\text{\AA}$  component incident is about 30% greater than the total intensity produced by irradiation with the  $7665\text{\AA}$  component. In this region of pressure, the contribution to the total fluorescent light arising from sensitized fluorescence is negligible. Therefore, the observed resonance fluorescence will depend on the relative absorption of the two wavelengths in this region. The absorption coefficient of the  $7665\text{\AA}$  component is twice that of the  $7699\text{\AA}$  component, leading to a lower total fluorescence with the shorter wavelength.

The minima in the two curves occurring at  $1 \times 10^{-3}$  Torr are due to

TABLE 3

Total Intensity in Sensitized Fluorescence Induced  
by Potassium - Potassium Collisions.

Temperature °K	Pressure (Torr)	Total Intensity 7665Å Incident	Total Intensity 7699Å Incident
350	$3.3 \times 10^{-6}$	20.0	26.5
363	$9.4 \times 10^{-6}$	19.5	26.0
373	$2.0 \times 10^{-5}$	20.5	26.5
383	$4.0 \times 10^{-5}$	22.0	25.0
393	$8.2 \times 10^{-5}$	21.5	23.5
403	$1.6 \times 10^{-4}$	18.5	21.5
418	$4.0 \times 10^{-4}$	15.0	16.5
438	$1.2 \times 10^{-3}$	11.2	12.4
448	$2.0 \times 10^{-3}$	17.0	14.0
457	$3.2 \times 10^{-3}$	27.5	18.4
468	$7.0 \times 10^{-3}$	26.5	18.5
479	$1.0 \times 10^{-2}$	24.0	18.2
493	$1.6 \times 10^{-2}$	20.5	16.4
513	$3.6 \times 10^{-2}$	15.4	14.2
533	$7.8 \times 10^{-2}$	7.8	7.0

All intensities given in arbitrary units.

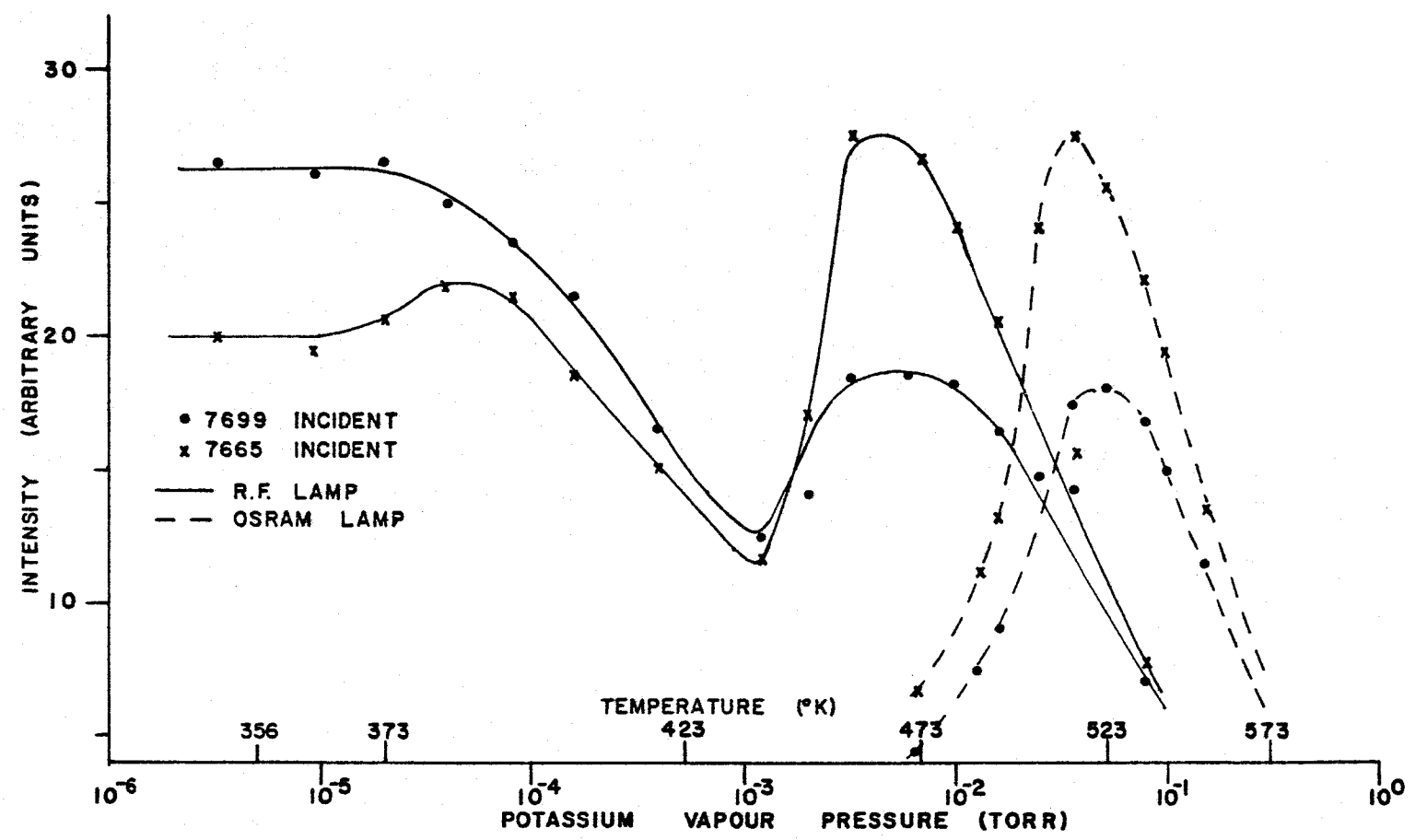


figure (15) The Variation of the Total Fluorescent Intensity With Potassium Vapour Pressure

the decreased efficiency of the absorption process due to the broadening of the absorption line in the sample due to the increase in pressure. From this point, sensitized fluorescence contributes an appreciable fraction of the total fluorescent intensity. Radiation diffusion sets in leading to volume fluorescence at about  $5 \times 10^{-3}$  Torr, which produces a maximum in observed intensity. As the potassium vapour pressure increases, surface fluorescence begins to predominate, leading to gradually vanishing intensities at the point of observation with either D line incident. In general, these curves agree very well with the findings of Hoffmann and Seiwert (1960).

Plotted for comparison is a set of curves obtained by Brockman (1962) who used an Osram potassium spectral lamp. Their peaks have been normalized to the intensity peaks produced by the R.F. Lamp. Only one maximum is in evidence, and it is displaced by one order of magnitude towards higher potassium vapour pressures from the second set of maxima produced by the R.F. Lamp. From the shape and position of these curves, the advantages offered by the R.F. Lamp in the region of low potassium vapour pressure are immediately apparent.

### Sensitized Fluorescence Induced by Potassium - Argon Collisions.

In order to study collisions of the second kind between potassium and argon, a fixed vapour pressure of potassium was established and various amounts of argon were admitted to the fluorescence cell. The intensity ratios  $\eta_1$  and  $\eta_2$  were then determined for each value of argon pressure. The experimental procedure was much the same as that used in the study of pure potassium. In this case, the variable factor was the density of argon atoms, rather than of potassium vapour.

The choice of a particular potassium vapour pressure depends on several factors. The ratio of potassium density to argon density must not be so low that the transitions of interest occur too rarely to be observed. This ratio must also be large enough so that quenching of the excited potassium atoms by impurities in the argon or by the argon itself does not reach significant proportions. Conversely, if the potassium vapour density rises above  $3 \times 10^{-4}$  Torr, imprisonment of radiation may present a problem. Finally, the density ratio of argon to potassium must be so large at all argon pressures that there will be no significant contribution to the intensity ratios from collisions between potassium atoms.

After preliminary experimental runs at 361°K, 373°K, 423°K and 473°K, a temperature of 373°K corresponding to a potassium vapour pressure of  $2 \times 10^{-5}$  Torr was chosen as the most likely to fulfill all of the above conditions. At 361°K ( $8 \times 10^{-6}$  Torr) quenching by impurities in the argon completely blocked fluorescence above 1.0 Torr argon pressure. At 423°K and 473°K, radiation imprisonment was a dominant factor.

The argon used in these experiments was obtained from the Linde Air Products Co. and was specified to contain less than 20 parts per

million of gaseous impurities. Commercial argon, in a steel tank obtained from Liquid Carbonic Canadian Co., was also used and gave results indistinguishable from those obtained with the spectroscopically pure gas.

The intensity ratios  $\eta_1$  and  $\eta_2$  obtained under these conditions are shown in Table 4. The experimental results in the pressure range 1.0 to 30 Torr are, on the whole, not as reproducible as those obtained throughout the potassium experiments. This is at least partly due to the low potassium vapour density and to the fact that the argon appeared to dissolve in the potassium, lowering its vapour pressure. Because of this complication, the intensity ratios tended to depend on whether argon pressures were increasing or decreasing, and in order to reduce this effect, it was necessary to heat the potassium to 473° K and out-gas frequently.

Figure (16) shows a plot of  $\eta_1$  and  $\eta_2$  against argon pressure. It can be seen that  $\eta_1$  reached a steady value of 0.600 very quickly while  $\eta_2$  approached 1.60 more slowly. The low pressure results which are lost in this plot are shown semi - logarithmically in figure (17). The low - pressure ratios were very reproducible because of the relatively small quenching effect.  $\eta_1$  and  $\eta_2$  become equal to one another as the argon pressure decreases to 1.0 Torr, in a manner similar to that observed for potassium collisions. Various values of  $\eta_1$  and  $\eta_2$  were read off these plots and substituted in equations (20) and (21) to calculate the collision numbers. These are listed in Table 5 and plotted against argon pressure in figure (18).

It can be seen that  $Z_1$  and  $Z_2$  vary linearly with pressure at pressures above 20 Torr. At very low pressures, (below 1.0 Torr)  $Z$

TABLE 4

Intensity Ratios in Sensitized Fluorescence Induced  
by Potassium - Argon Collisions.

Pressure of Argon (Torr)	$\eta_1$ $I_1/I_2$	$\eta_2$ $I_2/I_1$		Pressure of Argon (Torr)	$\eta_1$ $I_1/I_2$	$\eta_2$ $I_2/I_1$
$1.0 \times 10^{-3}$	0.0065	0.0063		7.6	0.621	0.790
$1.5 \times 10^{-3}$	0.0123	0.0074		12.0	0.623	0.826
$3.1 \times 10^{-3}$	0.0137	0.0175		12.4	0.608	0.927
$3.2 \times 10^{-3}$	0.0135	0.0109		17.7	0.608	0.954
$5.2 \times 10^{-3}$	- - -	0.0188		24.9	0.694	0.988
$6.0 \times 10^{-3}$	0.0202	0.0184		25.2	0.669	1.041
$7.0 \times 10^{-3}$	0.0218	0.0247		29.0	0.516	1.056
$1.1 \times 10^{-2}$	0.0177	0.0177		30.0	0.554	1.065
$1.2 \times 10^{-2}$	0.0242	0.0230		36.0	0.598	1.088
$2.2 \times 10^{-2}$	0.0274	0.0233		48.0	0.584	1.121
$5.9 \times 10^{-2}$	0.0539	0.0519		50.0	0.623	1.160
$1.0 \times 10^{-1}$	0.0839	0.0816		75.5	0.597	1.275
$1.9 \times 10^{-1}$	0.134	0.138		99.8	0.534	1.308
$3.2 \times 10^{-1}$	0.180	0.176		147	0.612	1.346
$4.6 \times 10^{-1}$	0.247	0.255		197	0.626	1.463
1.0	0.362	0.371		260	0.586	1.451
1.4	0.457	0.485		298	0.599	1.575
2.6	0.519	0.556		347	0.605	1.519
3.1	0.501	0.652		397	0.607	1.525
3.5	0.625	0.638		438	0.611	1.498
4.3	- - -	0.639		495	0.569	1.566
7.2	- - -	0.788		539	0.577	1.599



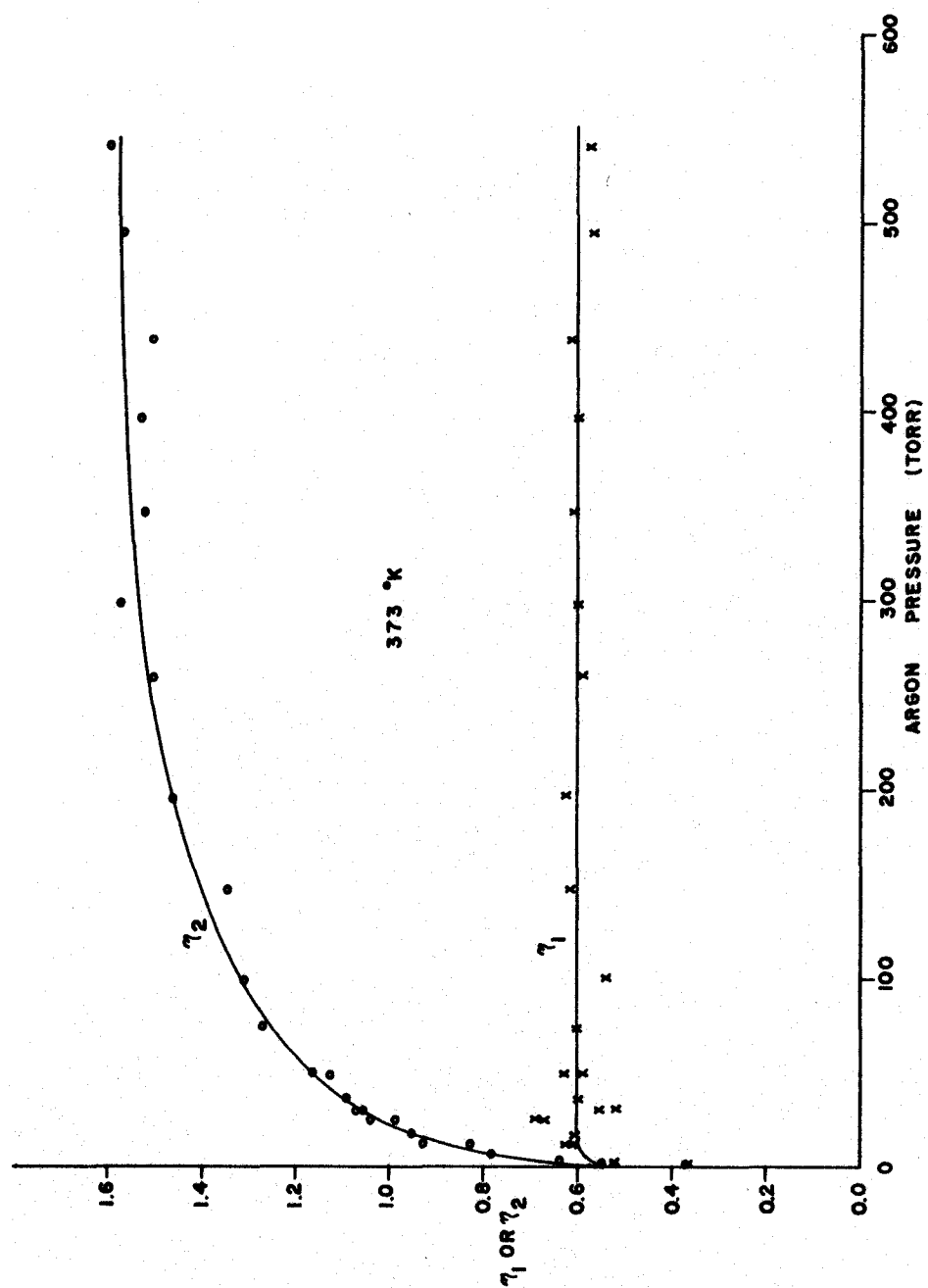


figure (16) The Variation of  $\gamma_1 = I_1/I_2$  and  $\gamma_2 = I_2/I_1$  With Argon Pressure

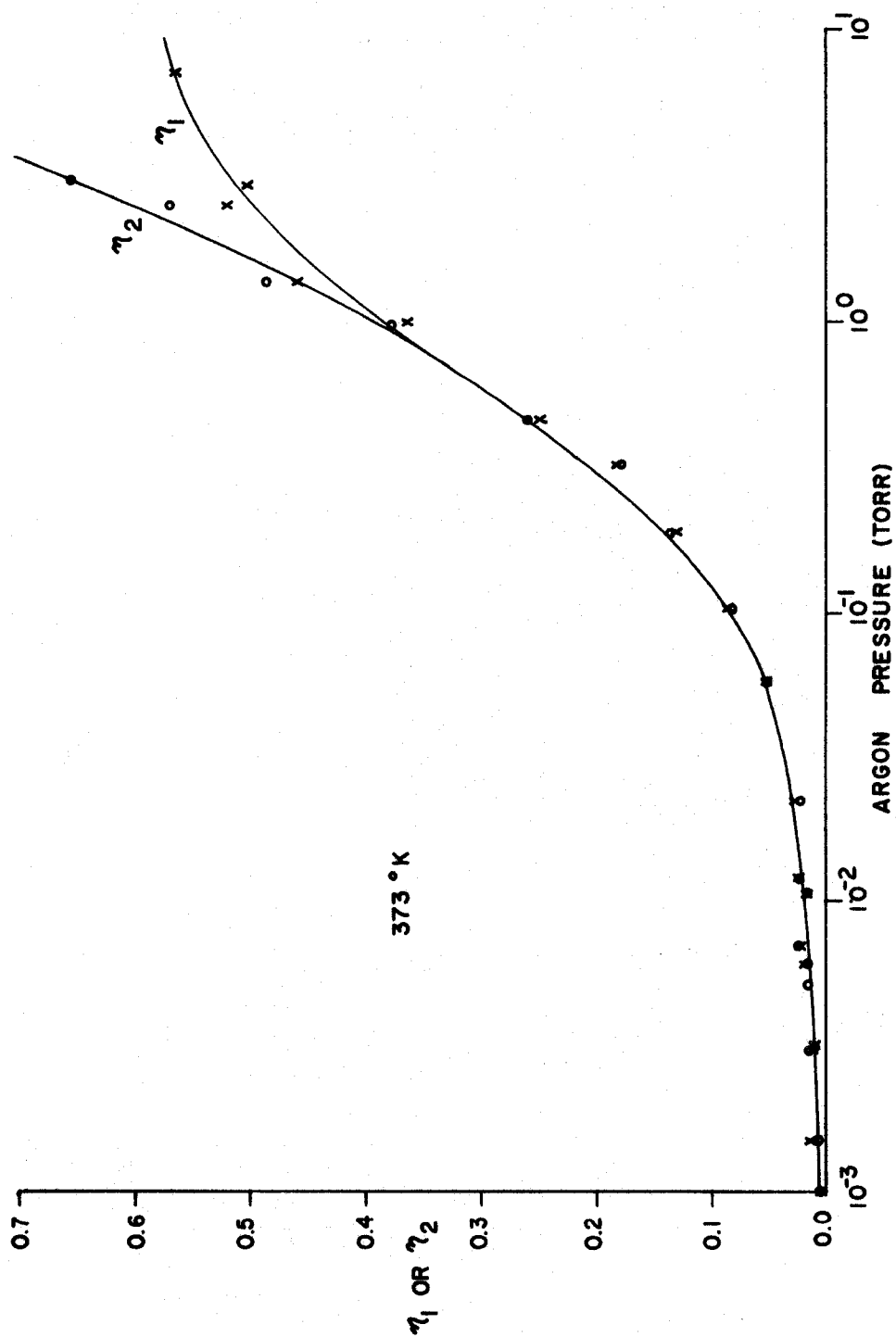


figure (17) A Semi - Logarithmic Plot of  $\eta_1 = I_1/I_2$  and  $\eta_2 = I_2/I_1$  With Argon Pressure

TABLE 5

Collision Numbers in Sensitized Fluorescence Induced by  
Potassium - Argon Collisions

Pressure of Argon (Torr)	$\eta_1 = I_1/I_2$	$\eta_2 = I_2/I_1$	$\overset{Z_1}{2P_{1/2}} \rightarrow \overset{Z_2}{2P_{3/2}}$ Coll/atom/sec	$\overset{Z_2}{2P_{3/2}} \rightarrow \overset{Z_1}{2P_{1/2}}$ Coll/atom/sec
$3.0 \times 10^{-3}$	0.014	0.014	$5.46 \times 10^5$	$5.46 \times 10^5$
$1.0 \times 10^{-2}$	0.021	0.021	$8.25 \times 10^5$	$8.25 \times 10^5$
$3.0 \times 10^{-2}$	0.029	0.029	$1.15 \times 10^6$	$1.15 \times 10^6$
$1.0 \times 10^{-1}$	0.083	0.083	$3.30 \times 10^6$	$3.30 \times 10^6$
$2.0 \times 10^{-1}$	0.138	0.138	$6.15 \times 10^6$	$6.15 \times 10^6$
$6.0 \times 10^{-1}$	0.278	0.278	$1.48 \times 10^7$	$1.48 \times 10^7$
1.0	0.332	0.332	$1.92 \times 10^7$	$1.92 \times 10^7$
2.0	0.490	0.530	$4.10 \times 10^7$	$3.90 \times 10^7$
3.0	0.550	0.620	$5.61 \times 10^7$	$5.20 \times 10^7$
4.0	0.583	0.660	$6.54 \times 10^7$	$6.05 \times 10^7$
5.0	0.598	0.713	$7.64 \times 10^7$	$6.89 \times 10^7$
6.0	0.600	0.750	$8.40 \times 10^7$	$7.35 \times 10^7$
8.0	0.600	0.812	$9.75 \times 10^7$	$8.15 \times 10^7$
10	0.600	0.863	$1.10 \times 10^8$	$8.92 \times 10^7$
20	0.600	0.988	$1.50 \times 10^8$	$1.13 \times 10^8$
30	0.600	1.054	$1.78 \times 10^8$	$1.29 \times 10^8$
50	0.600	1.157	$2.32 \times 10^8$	$1.63 \times 10^8$
100	0.600	1.308	$3.73 \times 10^8$	$2.47 \times 10^8$
150	0.600	1.380	$4.92 \times 10^8$	$3.19 \times 10^8$
200	0.600	1.433	$6.34 \times 10^8$	$3.99 \times 10^8$
250	0.600	1.474	$7.89 \times 10^8$	$4.93 \times 10^8$
300	0.600	1.504	$9.46 \times 10^8$	$5.92 \times 10^8$

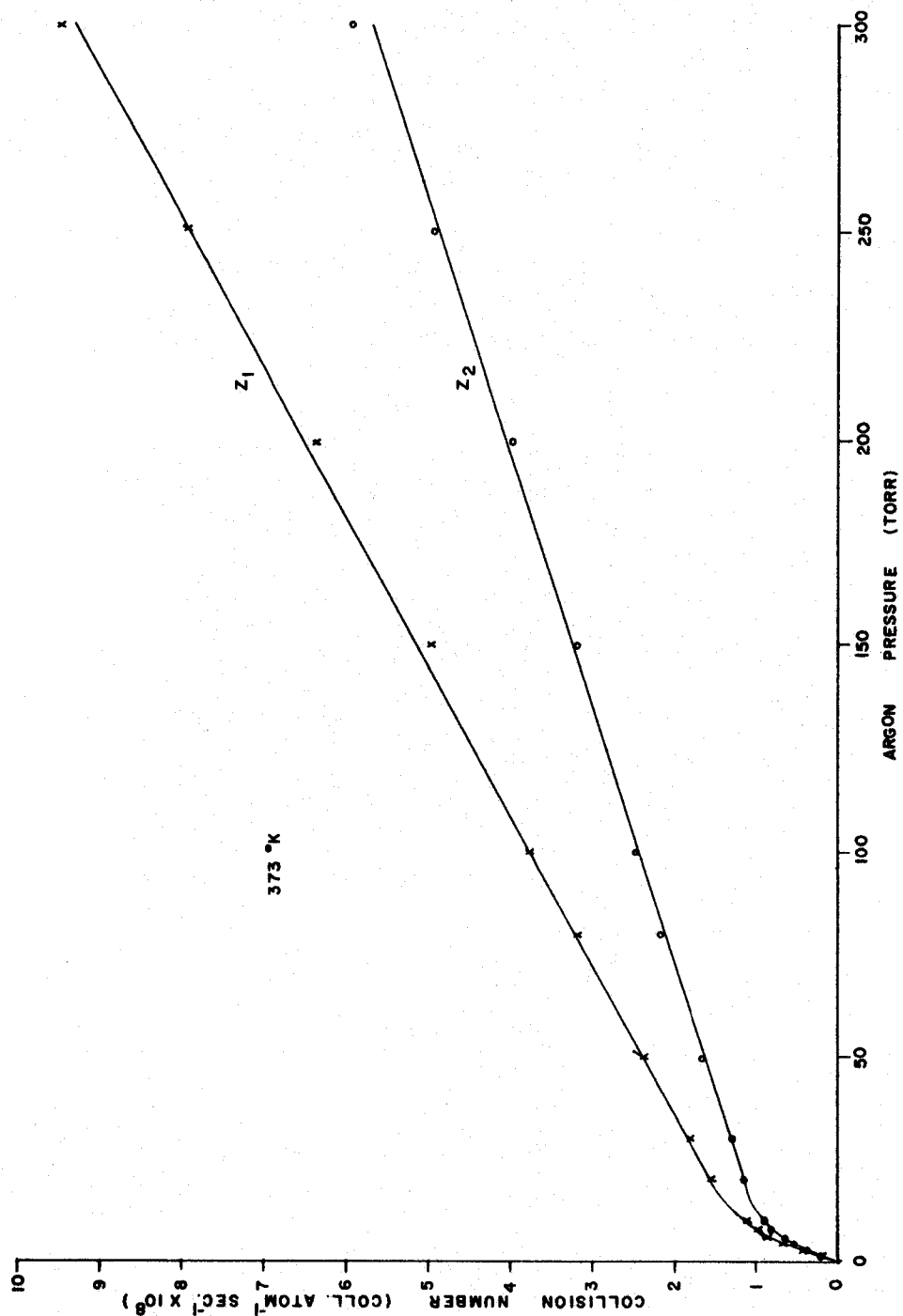


figure (18) The Variation of  $Z_1( {}^2P_{1/2} \rightarrow {}^2P_{3/2} )$  and  $Z_2( {}^2P_{3/2} \rightarrow {}^2P_{1/2} )$  With Argon Pressure

varies linearly with pressure but at a different rate. The two regions are connected at intermediate pressures by a non linear portion of the curves for  $Z_1$  and  $Z_2$ . The portions of the graph, corresponding to high pressures, when extrapolated to low argon pressures, do not pass through the origin. This would indicate that the collision cross sections  $Q_1$  and  $Q_2$  are pressure dependent as shown by the following equations:

$$Q_1 = \left( 8.70 \times 10^{-17} + \frac{3.15 \times 10^{-15}}{P} \right) \sqrt{T}$$

$$Q_2 = \left( 5.14 \times 10^{-17} + \frac{2.52 \times 10^{-15}}{P} \right) \sqrt{T}$$

At higher pressures the dependence on pressure would be reduced. At 200 Torr and 373°K, the cross sections become:

$$Q_1 = 1.98 \times 10^{-15} \text{ cm}^2$$

$$Q_2 = 1.23 \times 10^{-15} \text{ cm}^2$$

which are comparable to the gas kinetic cross sections. Quenching, if present, would cause a change in the constants involved in these two equations.

The low pressure curve for  $Z$  is shown in figure (19). In the pressure range 0.0 to 1.0 Torr,  $Z_1$  and  $Z_2$  are equal and vary linearly with pressure, as in the case of very low pressures of pure potassium vapour. Above 1.0 Torr, the curves for  $Z_1$  and  $Z_2$  separate and gradually assume the shapes shown in figure (18).

Treating the linear variation as outlined for the potassium results, the cross section for potassium - argon collisions at low pressures is given by :

$$Q = 7.25 \sqrt{T} \times 10^{-16} \text{ cm}^2$$

At 373°K,  $Q = 1.4 \times 10^{-14} \text{ cm}^2$

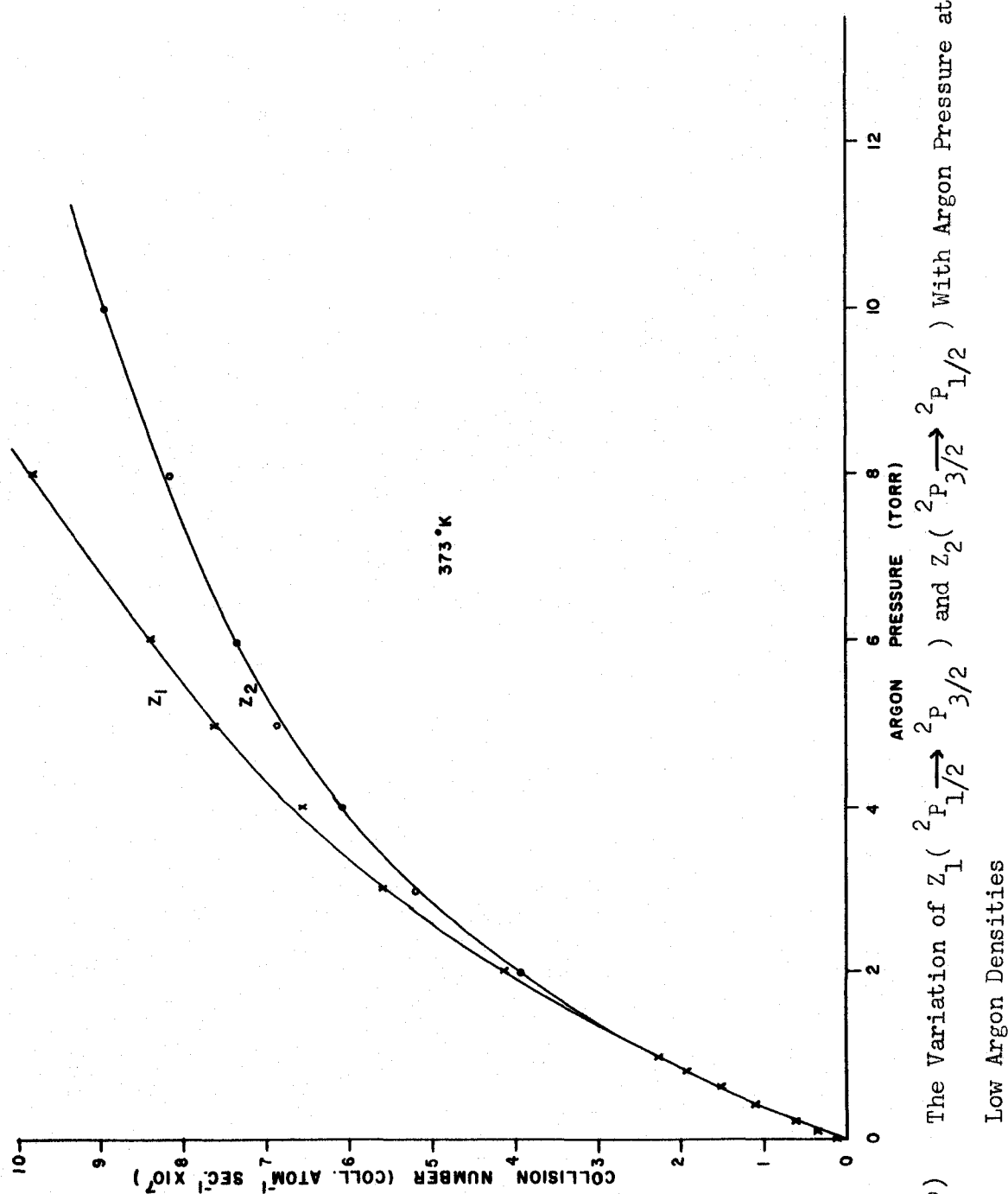


figure (19) The Variation of  $Z_1( \text{}^2P_{1/2} \rightarrow \text{}^2P_{1/2} )$  and  $Z_2( \text{}^2P_{3/2} \rightarrow \text{}^2P_{1/2} )$  With Argon Pressure at Low Argon Densities

## V THE RELATIONSHIP BETWEEN $Q_1$ AND $Q_2$ FOR INELASTIC COLLISIONS

In both the pure potassium and potassium - argon systems, the intensity ratio curves merge at some specific pressures, implying equality of the two cross sections for the upward and downward transitions. At those pressures the effective statistical weights of the  $^2P_{1/2}$  and  $^2P_{3/2}$  levels must therefore be the same. Such a condition will result if two assumptions are made. If the total angular momentum of the two colliding atoms along the collision axis is conserved and if the orientation of the ground state atom remains unchanged, then equality of statistical weights will be achieved. The orientation of the ground state does not seem to affect the interaction since similar behaviour at low pressures is observed with potassium,  $^2S_{1/2}$ , and argon,  $^1S_0$ . If the ground state is not an S state, however, the conservation of angular momentum may also include the contribution due to ground - level orientation.

If the expression obtained for the cross sections in both systems at high and low pressures are compared, several facts of interest are brought to light. In both systems, at low pressures, where it is assumed that the total angular momentum is conserved, the cross section varies only with the relative velocity ( $\sqrt{T}$ ) of the colliding atoms. At high pressures, the cross sections are no longer equal to one another and vary inversely with the pressure and directly with relative velocity. Thus it would appear that there are two possible mechanisms for energy transfer. One is characterized by angular momentum conservation along the collision axis, velocity dependence

and relatively high efficiency. The other is characterized by an inverse dependence on pressure and relatively low efficiency.

The following expression may be derived from the ideal gas law, which shows the relationship between pressure, temperature, and atomic density.

$$N = 9.656 \frac{P \text{ (Torr)}}{T} \times 10^{18} \frac{\text{atoms}}{\text{cc}}.$$

The linear pressure dependence of the collision numbers may be interpreted as a variation with the product of atomic density and absolute temperature or kinetic energy. Considering this fact, it seems that whenever a two - phase system is involved, such as potassium, where the pressure is a function of the temperature, it will be impossible to observe a true linear variation of collision numbers with pressure in pressure ranges where the temperature is varying rapidly. A straight line was obtained for  $Z$  at low potassium pressures only because of the slow variation of temperature in that pressure region. For this reason, if the collision mechanism is the same at high pressures in both the potassium and potassium - argon systems it should not be possible to observe an unperturbed linear variation of  $Z_1$  and  $Z_2$  at high potassium vapour pressures.



## VI CONCLUSIONS

Sensitized fluorescence in potassium induced by potassium - potassium and potassium - argon collisions was investigated for the first time at very low potassium densities. It appears that in both systems, the cross sections  $Q_1$  ( $4^2P_{1/2} \rightarrow 4^2P_{3/2}$ ) and  $Q_2$  ( $4^2P_{3/2} \rightarrow 4^2P_{1/2}$ ) are identical at low pressures. For potassium - potassium collisions, systems, the cross sections  $Q_1$  ( $4^2P_{1/2} \rightarrow 4^2P_{3/2}$ ) and  $Q_2$  ( $4^2P_{3/2} \rightarrow 4^2P_{1/2}$ )

$$= 6.6 \times 10^{-12} \text{ cm}^2 \text{ at about } 400^\circ\text{K}$$

and for potassium - argon collisions,

$$Q = 7.25 \times 10^{-15} \sqrt{T}$$

$$= 1.4 \times 10^{-4} \text{ cm}^2 \text{ at } 373^\circ\text{K}$$

Thus, at low pressures, the cross sections depend upon the relative velocity of the colliding atoms. Also the collision numbers depend upon the product of atomic density and the kinetic energy (or temperature). The efficiency of the potassium - potassium collisions is much greater than that of the potassium - argon collisions.

The fact that the cross sections for the upward and downward transitions are equal is explained by the assumption that the component of the total angular momentum of the colliding atoms along the collision axis,  $\Sigma J_z$ , is conserved ( $\Delta \Sigma J_z = 0$ ) during an inelastic collision, and that the orientation of the ground state atom ( $^2S_{1/2}$  or  $^1S_0$ ) does not change.

At higher pressures,  $Q_1 \neq Q_2$  in either system. The cross sections are much smaller and vary inversely with the pressure and directly with the relative velocity. There, the collision numbers are

expected to vary linearly with pressure, but much more slowly than at low pressures. This variation has been demonstrated experimentally for potassium - argon collisions (fig 18). No such linear variation could be observed at high potassium vapour pressures because of the temperature dependence of the collision numbers, and of the fact that potassium pressure is a function of temperature. Further complications are also introduced by the presence of radiation imprisonment.

For potassium - argon collisions at pressures above 20 Torr:

$$Q_1 = \left( 8.70 \times 10^{-17} + \frac{3.15 \times 10^{-15}}{P} \right) \sqrt{T}$$

$$= 1.98 \times 10^{-15} \text{ cm}^2 \text{ at 200 Torr and } 373^\circ \text{K},$$

and  $Q_2 = \left( 5.14 \times 10^{-17} + \frac{2.52 \times 10^{-15}}{P} \right) \sqrt{T}$

$$1.23 \times 10^{-15} \text{ cm}^2 \text{ at 200 Torr and } 373^\circ \text{K}$$

In this pressure range, the cross sections for collisions of the second kind are of the same order of magnitude as the gas kinetic cross sections and  $Q_1$  is no longer equal to  $Q_2$ . These two facts would imply that the energy transfer might proceed by different mechanisms at low and high pressures.

The cross sections for potassium measured in this investigation are much larger than those of Hoffmann and Seiwert (1961). These authors carried out their experiments in the presence of radiation diffusion, and employed Holstein's theory to correct for the diffusion effects. No such corrections were required in this investigation. Their measurements were taken in that region of potassium vapour pressure in which the cross sections seem to be the result of a collision mechanism different from that which dominates the low pressure region. In view of the fact that the cross sections for potassium - argon collisions at high and low pressures differed by an order of

magnitude, it may well be that the measurements made by Hoffmann and Seiwert were the result of the less efficient pressure dependent mechanism.

## BIBLIOGRAPHY

- Barrat, J. P. 1959. J. Phys. Radium. (5) 20: 541.  
 -----, 1959. J. Phys. Radium. (6) 20: 633.  
 -----, 1959. J. Phys. Radium. (7) 20: 42.  
 Beutler, H. and Josephy, B. 1929. Z. Phys. 53: 747.  
 Brockman, I. H. 1962. Private Communication.  
 -----, 1963. Private Communication.  
 Carlo, G. and Franck, J. 1922. Z. Phys. 11: 161.  
 Compton, K. 1923. Phil. Mag. 45: 752.  
 Ditchburn, R. W. and Gilmour, J. O. 1941. Rev. Mod. Phys. 13: 310.  
 Franck, J. 1929. Naturwissenschaften 14: 211.  
 Gerard, V. B. 1962. J. Sci. Instrum. 39: 217.  
 Hoffmann, K. and Seiwert, R. 1960. Exper. Tech. der Phys. 4: 161.  
 Hoffmann, K. and Seiwert, R. 1961. Ann. Phys. (7) 7: 71.  
 Holstein, T. 1947. Phys. Rev. 72: 1212.  
 Killian, T. J. 1926. Phys. Rev. 27: 578.  
 Krause, L. and Neville, R. 1963. J. Sci. Instrum. (6) 34: 698.  
 Milne, E. 1926. J. lond. Math. Soc. 1: 1.  
 Neilsen, R. and Wright, N. 1930. J. Opt. Soc. Amer. 20: 27.  
 Rae, A. G. A. 1963. Private Communication.  
 Thangaraj, M. 1948. Ph.D Thesis, University of Toronto.  
 Wood, R. W. 1905. Phil. Mag. 10: 513.

## VITA AUCTORIS

The author was born in 1940, in Windsor, Ontario. He attended Assumption College High School from 1953 to 1957. In 1958, the author enlisted as a Technical List officer in the Royal Canadian Air Force, under the Regular Officer's Training Plan, and was enrolled in the Honours Chemistry and Physics programme at Assumption University of Windsor. In 1961, he was honourably released from service and continued his studies under an in - course scholarship, obtaining his B.Sc. degree in 1962. In the same year, he was awarded the Society of Chemical Industry Merit Award Key in Chemistry, and a National Research Council of Canada graduate bursary. In 1962, the author began graduate studies in Physics at the University of Windsor.